



UiT The Arctic University of Norway

Faculty of Science and Technology,
Department of Physics and Technology

Performance and Future Potential of Solar Photovoltaics in Arctic Settlements

Vemund Nygaard Mathiesen

EOM-3901 Master's thesis in Energy, Climate and Environment

December 2020

Abstract

Data from a solar photovoltaic (PV) installation on Svalbard Airport Longyear has been analyzed to investigate performance of solar photovoltaics in the Arctic. Results show that the average capacity factor at the facility is 5.6 % after its first two full years of production. While the production in the winter is zero, monthly capacity factors are observed to be as high as 16 % in the summer. On peak days, capacity factors of more than 30 % are observed. Predictions show that the installation will save around 800 000 NOK during its 25-year lifetime, while also reducing emissions by 1064 tons CO₂ equivalents.

The data from Svalbard Airport Longyear was paired with energy consumption data from Longyearbyen, to design systems with different levels of reliance on solar energy. Simulations show that full solar reliance in the summer-season is feasible. It requires an installation of 86.3 MW_p solar PV, and 2.76 GWh of storage with 60 % round-trip efficiency. Estimations show a potential return on investment of 7.71 % after 25 years, saving 163 Million NOK. The emission reduction from the system would be 20 365 tons CO₂ equivalents.

The fragile power grids of arctic settlements have few links in the system that can equalize load fluctuations. Introduction of intermittent solar PV on even a private scale is therefore advised against until energy storage capacity is developed. Compressed air energy storage is suggested as an option for settlements on Svalbard because the required infrastructure already exists.

Because of the high heat demand in arctic settlements, efficiency of the fossil generators is higher than global average. Longyearbyen sees efficiencies of 50.1 % in the coal power plant, and Ny-Ålesund up to 76 % for its diesel generator. Paired with low solar utilization, the climate impact from installing PV in the Arctic is lower than in areas with low fossil efficiency and high solar utilization.

Acknowledgements

I would like to thank the University of Tromsø, and my classmates there, for three unforgettable years. The opportunity to experience a semester in Longyearbyen, I also owe to UiT. My supervisor, Matteo Chiesa, also deserves a thanks for pointing me in the right direction with my project paper and this master thesis.

I want to express thanks to my family and friends as well, and a special thank you to Hilde Kari, for providing me with the freedom that I sometimes require for my pointless adventures.

Contents

- Abstract i
- Acknowledgementsiii
- List of Figures ix
- List of Tables..... xi
- 1 Introduction 1
 - 1.1 Idea Behind Project 2
 - 1.2 Objective..... 2
- 2 Theory 3
 - 2.1 The Arctic 3
 - 2.1.1 Climate 3
 - 2.1.2 Axial Tilt 3
 - 2.1.3 Svalbard..... 5
 - 2.2 Energy in the Arctic..... 6
 - 2.2.1 Longyearbyen..... 8
 - 2.2.2 Ny-Ålesund 8
 - 2.3 Solar Photovoltaics 9
 - 2.3.1 The Photovoltaic Effect..... 9
 - 2.3.2 Solar Radiation 10
 - 2.3.3 Atmospheric Effects 11
 - 2.3.4 Global Horizontal Irradiance and Albedo 12
 - 2.3.5 Standard Testing Conditions 13
 - 2.3.6 Effect of Temperature 13
 - 2.3.7 Bifacial Solar Panels 13
 - 2.3.8 Solar Tracker Systems..... 14
 - 2.3.9 Global Market 14

2.4	Energy Storage	15
2.4.1	Round-Trip Efficiency	15
2.4.2	Batteries.....	16
2.4.3	Heat Storage	16
2.4.4	Compressed Air Energy Storage	16
2.4.5	Hydro and Pumped Hydro Storage	17
2.5	Capacity Factor.....	18
3	Method	21
3.1	Svalbard Airport Solar Facility.....	21
3.1.1	Sun Conditions	22
3.1.2	Weather	24
3.1.3	Solar Panels	25
3.1.4	Degradation	26
3.1.5	Inverters.....	27
3.1.6	Orientation of Panels	29
3.1.7	Production Data.....	30
3.2	Previous Work	33
3.3	Simulation.....	33
3.4	Analysis Tool.....	33
4	Findings.....	35
4.1	Performance of PV in the Arctic	35
4.1.1	Capacity Factor	35
4.1.2	Optimal Installation Configuration	40
4.2	Improvement Suggestions	42
4.2.1	Tilt	43
4.2.2	Bifacial Technology	43

4.2.3	Tracking Systems	44
4.3	Simulation of Solar PV Systems	44
4.3.1	Energy Profile	44
4.3.2	Full Solar Dependency	47
4.3.3	Peak Load Energy Production and Storage	50
4.3.4	Summer-Only Solar Dependency	51
4.3.5	Combining Summer Solar and Peak Storage	54
4.4	Cost of Energy in the Arctic	56
4.4.1	Cost of Energy Storage	57
4.4.2	Cost of Solar Photovoltaics	57
4.5	Economic Impact	59
4.5.1	Svalbard Airport	59
4.5.2	Private Installations	59
4.5.3	Full Solar Dependency	61
4.5.4	Summer-Only Solar Dependency	61
4.6	Climate Impact	62
4.6.1	Svalbard Airport	64
4.6.2	Private installations	65
4.6.3	Full Solar Dependency	65
4.6.4	Summer-Only Solar Dependency	65
4.7	Discussion	66
5	Conclusion	69
6	Sources	71

List of Figures

Figure 1: Global temperature increase since the industrial revolution [2]..... 1

Figure 2: The axial tilt and seasons of the earth [9] 4

Figure 3: Daily hours of sun per day, based on latitude and date [10]..... 5

Figure 4: Svalbard’s location in the Barents Sea north of Scandinavia [12] [13]..... 6

Figure 5: Efficiency vs. Load for diesel generators [17]..... 7

Figure 6: Structure of a solar PV cell. The emitter is negatively doped, while the base is positively doped. The two form a PN-junction. [25] 9

Figure 7: Spectral irradiance for AM 0, AM 1.5 Direct and AM 1.5 GHI [29]..... 11

Figure 8: Air Mass with the simplified and exact method 12

Figure 9: Global solar PV capacity from 2000 to 2019 [37]..... 14

Figure 10: Compressed Air Energy Storage systems, simplified (a) and more efficient with heat storage (b) [42] 17

Figure 11: Avinor’s Greenhouse Gas Emissions Related To Airport Operations For Each Emission Source [54] 21

Figure 12: 360 degree horizon as seen from Svalbard Airport. Included are the sun’s path at summer solstice, and spring and autumn equinox. Winter solstice is below the horizon [57] 23

Figure 13: Average cloud cover at Svalbard Airport since 1980 [58] 24

Figure 14: Highest and Lowest Average Temperatures at Svalbard Airport since 1980..... 25

Figure 15: Expected degradation of the solar PV panels at Svalbard Airport 27

Figure 16: Calculation of the orientation of wall mounted solar panels [13] 29

Figure 17: Energy production for each of the 11 arrays at Svalbard Airport..... 31

Figure 18: Location of five of the arrays that track production data..... 32

Figure 19: Average monthly capacity factor for the 11 arrays in 2019 and 2020..... 36

Figure 20: Monthly capacity factor for each of the arrays 37

Figure 21: Demonstrating the shifted symmetry of the “10.0-3-M Hangar1_upperleft” and “10.0-3-M Hangar1_upright” arrays, compared to the “10.0-3-M Hangar1_center” array. Legend is wrong from the provider, and corrected in thesis 39

Figure 22: Maximum daily capacity factor since installation for all 11 arrays..... 40

Figure 23: Min and Max daily load in Longyearbyen in 2017, district heating [19]..... 45

Figure 24: Min and Max daily load in Longyearbyen in 2017, electricity [19]..... 45

Figure 25: Monthly energy production in 2017, Longyearbyen 46

Figure 26: Monthly energy production in 2017 and average capacity factor in 2019-20, Longyearbyen.....	47
Figure 27: Two-year simulation of a fully reliant solar PV Longyearbyen. Round-trip efficiency in storage 100%	48
Figure 28: Two-year simulation of a fully reliant solar PV Longyearbyen. Round-trip efficiency in storage 60%	49
Figure 29: Peak-Load energy supplied from solar PV. Efficiency of storage 60%	51
Figure 30: Daily capacity factor from March 1 st to September 30 th at Svalbard Airport.....	52
Figure 31: Simulation of a fully solar reliant Longyearbyen in 2020. Efficiency of storage 60%.....	53
Figure 32: Simulation of a fully solar reliant Longyearbyen in 2020. Energy produced from solar in March and September are sent to storage for peak-load supply in winter. Efficiency of storage 60%	55
Figure 33: Solar PV prices in December 2020. Tax-free prices, and modules only [62]	58
Figure 34: Annual savings in NOK per W_p installed in Longyearbyen for private installations	60

List of Tables

Table 1: Average capacity factor of some energy sources [48][50][47] 19

Table 2: Capacity factor of three different panel configurations 41

Table 3: Capacity factor of monocrystalline and polycrystalline panels 42

Table 4: Cost of solar PV per W_p , converted to NOK and accounting for taxes 58

Table 5: Carbon footprint from different energy sources [76 p. 1335] 62

Table 6: Carbon footprint from different energy sources in arctic conditions 64

Table 7: Climate impact of installing solar PV in the Arctic to replace electricity 65

1 Introduction

Global climate change is one of the greatest challenges that mankind faces. A global warming of 1.5 °C to 2 °C will lead to risks to health, livelihoods, food security, water supply, and economic growth [1]. Global mean temperatures are already 0.99 °C above the pre-industrial temperatures [2], and action must be made to limit the temperature increase. The Paris agreement just passed 5 years this December 12th, and to reach its goal of limiting the global warming to maximum 2 °C [3], urgent measures must be made.

The place on earth that experiences most global warming, is the arctic [4]. As seen in figure 1, temperatures have increased by well over 2 °C since the industrial revolution. The irony for arctic settlements, is that their energy supply is almost fully diesel and coal based, well-known contributors to the global climate change. For arctic settlements, replacing the fossil energy with renewable appears to be the obvious option to resolve this.

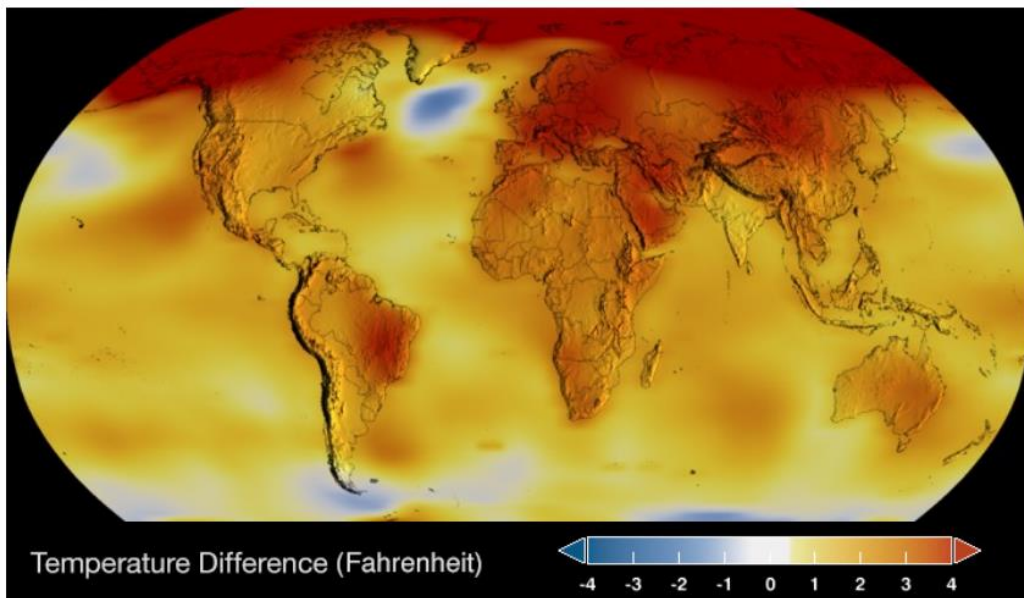


Figure 1: Global temperature increase since the industrial revolution [2]

1.1 Idea Behind Project

In the initial stages of the project, supervisor Matteo Chiesa presented a thought: The seasonal variation of occupants at polar research stations and settlement correlates well with the availability of the solar resource. Research stations have fewer occupants in the winter season, and larger settlements, like Longyearbyen see an influx of tourists in the summer season. Because of this correlation between the number of inhabitants, and the availability of the solar resource, groundworks began to explore whether this could make solar photovoltaics a viable option for energy supply at the settlements in question. It was quickly found that the energy demand of year-round manned settlements and research stations does not fluctuate as much as the population.

After this small set back, access to the production data from the fully operational, 138 kW, solar PV facilities of Svalbard Airport Longyear was granted by the manager, Carl Ivar Ianssen. This data is valuable as it is the first large-scale production data from solar PV in high-arctic conditions, just 1300 km from the North Pole. An interest was sparked to analyze this data and see how solar PV in the Arctic performs, and compare it to other locations. In addition, this analyzed data could be used to explore the possibilities of further developing larger scale PV projects in the Arctic.

1.2 Objective

The objective of the thesis is to establish how solar photovoltaics perform in arctic conditions, and how and if it can be integrated in the future arctic energy supply. The analyzing of future potential for solar photovoltaics in the arctic will include estimation of economic and climatic impact. Longyearbyen is the main focus of the thesis, because it is source of the data. The intent is, however, that the research will be applicable for other arctic settlements when transitioning to renewable energy.

2 Theory

2.1 The Arctic

The Arctic is the oceans and land masses surrounding the north pole [5]. There is no universally agreed definition of the Arctic, however there are definitions such as political, geographic, climatic, and geologic to name a few. From a solar photovoltaic perspective, it is natural to define the Arctic as the areas north of the polar circle. This frigid zone of the planet is one of two areas where midnight sun occurs in the summer, and the polar night in winter. The other area is inside the Antarctic Circle, at the opposite side of the planet, surrounding the South Pole. The polar circles are located at 66 degrees, 33 minutes, and 48 seconds north and south [6].

2.1.1 Climate

The climate of the Arctic varies enormously. Some regions in northern Scandinavia, like Lofoten in Northern Norway, experience annual median temperatures 5 °C [7]. Meanwhile, annual mean temperatures around the North Pole are observed to be as low as -20 °C [4]. Some of the huge differences in the arctic climate, can be attributed to ocean currents, in a region dominated by oceans [4]. Energy and water is transported to the Arctic through ocean currents and weather systems [4]. Both clouds and water vapor in the atmosphere in the Arctic traps heat. These effects make the Arctic, on average, more than 10 °C warmer than its southern counterpart, Antarctica [4].

2.1.2 Axial Tilt

The Earth's rotational plane around its own axis is tilted between 22.1 and 24.5 degrees from the rotational plane around the sun [8]. This obliquity variation changes over a 41000-year cycle and is one of the three Milankovitch cycles. The axial tilt of the Earth is now approximately 23.4 degrees and decreasing [8]. This tilt is the main reason the earth experiences seasons. The pole of the Earth facing away from the sun experience winter season, and the pole facing towards the sun has summer season, illustrated in figure 2.

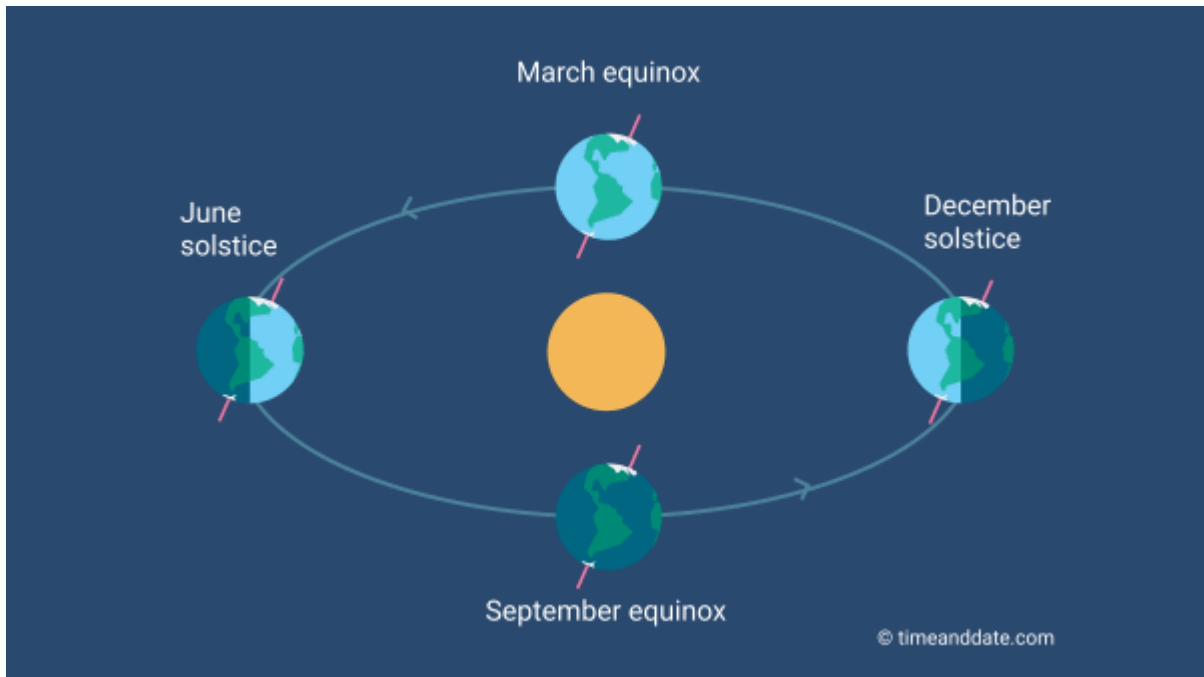


Figure 2: The axial tilt and seasons of the earth [9]

The polar circles are the approximate borders where the sun does not set at summer solstice and does not rise above the horizon at winter solstice. Their latitude can be easily approximated by subtracting the axial tilt from the total angle between the equator and the poles [6]:

$$\angle \text{Polar circle} = \angle \text{Pole} - \angle \text{Tilt} = 90^\circ - 23.4^\circ = 66.6^\circ$$

Meaning that the polar circles are located at approximately 66.6 degrees north and south.

Figure 3 is a visualization of the amount of daily hours of sun at different latitudes at certain days of the year. A symmetry can be observed between the start of the year and the end of the year, as well as in the north and south. The summer and winter season is opposite for the northern and southern hemisphere – When there is summer in the northern hemisphere, the southern has winter and vice versa. Also notable is the fact that the poles and equator have the same amount of annual sun hours. While the equator has 12 hours of sun each day, the poles have 24 hours for half the year, and zero hours for the rest of the year.

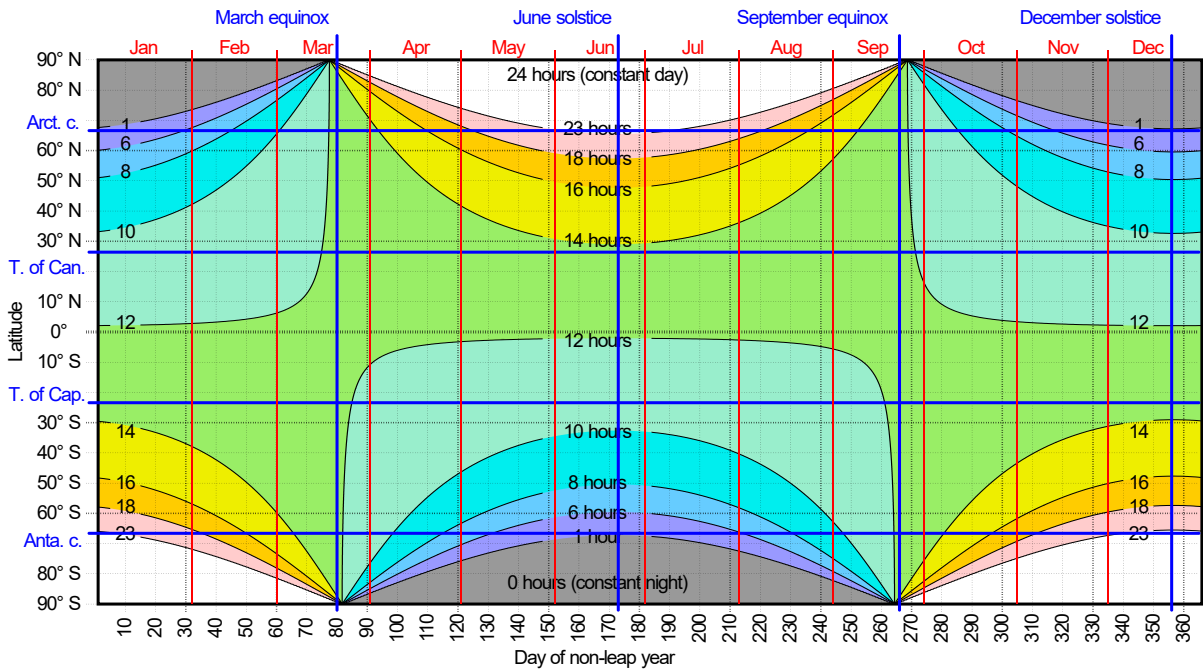


Figure 3: Daily hours of sun per day, based on latitude and date [10]

2.1.3 Svalbard

Svalbard is an archipelago under Norwegian Supremacy, as of the Svalbard Treaty signed in 1920 in the aftermath of World War 1 [11]. The archipelago consists of several islands, with Spitsbergen being the largest. Almost all inhabitants of Svalbard live in one of the two larger settlements on Spitsbergen; the mainly Russian/Ukrainian current mining settlement of Barentsburg, and the former miner settlement of Longyearbyen, which now has become a thriving tourism and research hotspot [5]. In addition, several small research stations like Ny-Ålesund, Hornsund and Bjørnøya has some inhabitants, mostly seasonal.



Figure 4: Svalbard's location in the Barents Sea north of Scandinavia [12] [13]

The remoteness of the Arctic Svalbard is illustrated in figure 4. It is located in the middle between mainland Norway and the North Pole. Stretching from 74 to 81 degrees north [14], the archipelago is well inside the Arctic Circle, and experience both midnight sun and polar night.

2.2 Energy in the Arctic

The harsh and inhospitable climate of the Arctic introduces many challenges in the energy sector that are specific to the region. The remoteness of most of the settlements in the Arctic means the settlements are reliant on off-grid energy solutions and are self-supplied with energy. In addition, the cold climate, especially winters, creates a substantial heat demand in the settlements.

Most polar settlements are supplied with energy from diesel generators and/or coal power plants. Barentsburg and Longyearbyen on Svalbard have coal power plants, supplied with locally mined coal. In addition, emergency diesel generators are present if needed. Smaller

settlements like Sveagruva and Ny-Ålesund have diesel generators. In Antarctica, diesel is the main fuel source, although a nuclear power plant powered the McMurdo Station in the 1960's and 1970's. It had to be shut down due to complications in the harsh climate [15].

Because the power grids in arctic settlements relies on few energy sources, they are vulnerable to rapid fluctuations in load. The energy production has few ways to regulate the load. Heavy load regulation damages the system in Longyearbyen, and Longyearbyen Lokalstyre is looking to expand the system with energy storage to help regulate this issue [16]. In the meantime, a ban on unregulated energy sources, like private wind and solar energy, has been suggested [16].

The efficiency of diesel generators is dependent on the load. The efficiency is best at 100% load and drops towards zero for 0% load [17]. Figure 5 illustrates this for generators from 5 to 200 kW. Operating diesel generators at low load levels for extended periods of time is damaging to the units, and generators are generally designed to operate at 70-100% load [18].

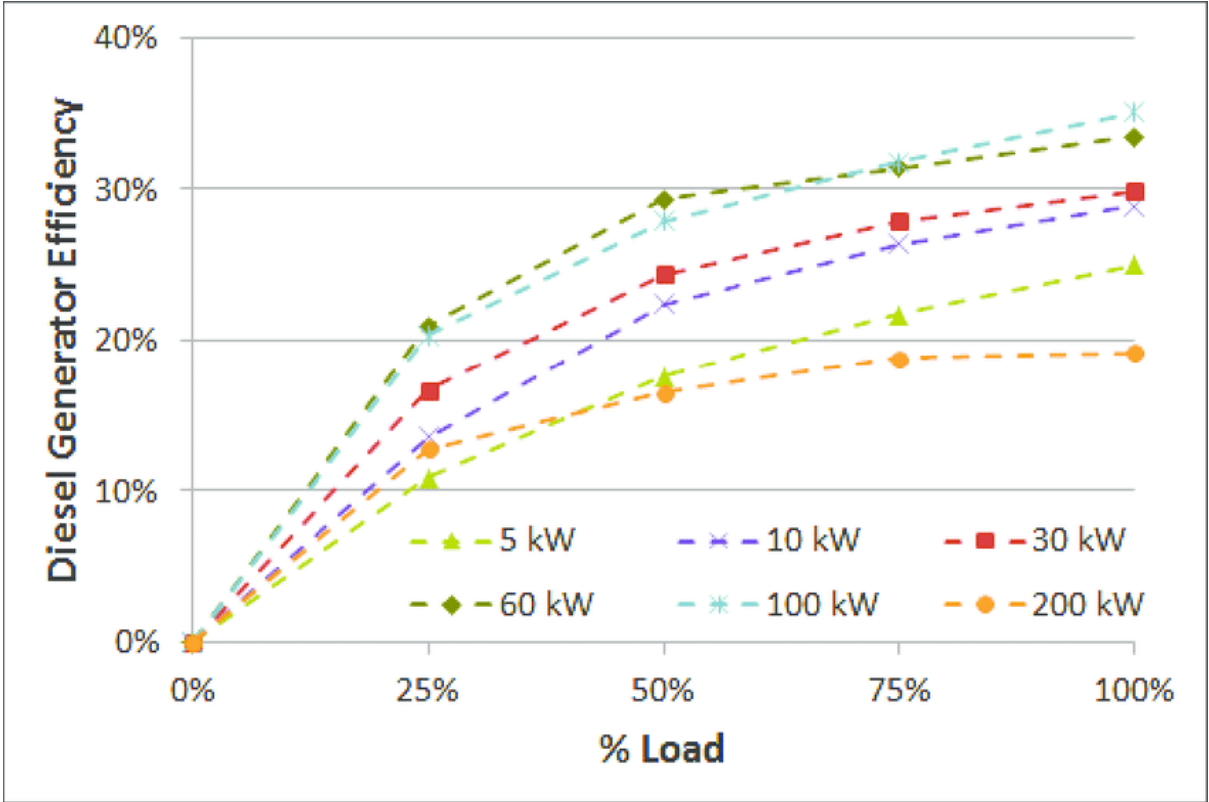


Figure 5: Efficiency vs. Load for diesel generators [17]

2.2.1 Longyearbyen

Longyearbyen is the largest settlement in the archipelago of Svalbard in the Barents Sea. The population is around 1600 [5]. The energy in Longyearbyen is mainly provided by a coal power plant operated by Longyearbyen Lokalstyre. It consists of two steam turbines with a theoretical power of 5.5 MW each, giving a total of 11 MW. In addition, a district heat generator is connected to one of the turbines, with a power of 22 MW [19 p. 20]. A treatment system that cleans the exhaust sets limitations to maximum production rate. The rated power of the power plant is therefore 7.5 MW in electricity and 16 MW for district heating [19 p. 20]. Annual energy production is around 110 000 MWh, 40 000 MWh of electricity and 70 000 MWh of district heating [19 p. 13]. In addition to the coal power plant, there are several backup generators. The reserve power near the city center has an installed effect of 5400 kW, with 3 1800 kW generators. They supply a stable power of 1500 kW each when operated [19 p. 22]. The backup generators were operational approximately 6 hours every day of the winter 2020. Not for backup purposes, but to meet the peak loads where the coal power plant did not supply sufficient energy [20].

2.2.2 Ny-Ålesund

Ny-Ålesund is an old coal miner's settlement in the northern parts of Spitsbergen, which was populated over 100 years ago. It is now a thriving research settlement, and by many considered the world's northernmost settlement. The population of Ny-Ålesund depends on the season. In 2007, the population approximately quintupled from the winter to the summer, from 30 to 150 [21]. It is reasonable to assume that this is because of favorable conditions for scientific research in the summer season. The energy in Ny-Ålesund is supplied by three identical Mitsubishi engines connected to a Stamford generator. The maximum load is 470 kW [22 p. 5]. Around 1000 m³, or 1 000 000 liters of fuel is consumed annually by the research settlement [22 p. 6]. The total efficiency of the diesel generator in Ny-Ålesund is 76% [22 p. 6], when including waste heat utilization. Diesel has a specific density of 0.85 kg/l [23], an energy density of 12 667 Wh/kg [24]. Total energy consumption can be calculated:

$$E_{annual} = 1\,000\,000\ l \cdot 0.85\ kg/l \cdot 12\,667\ Wh/kg = 8.183\ GWh$$

8.183 GWh of energy is consumed at the settlement each year.

2.3 Solar Photovoltaics

Solar photovoltaics (PV), converts incoming solar electromagnetic radiation into electric current, utilizing the photovoltaic effect. The photovoltaic effect is a physical and chemical phenomenon. When a surface with certain properties is exposed to electromagnetic radiation with sufficient energy, electrons of the atoms in the surface can be excited to an excited state. This excited state electron has gained an electric potential, which can be utilized in an electric circuit.

2.3.1 The Photovoltaic Effect

In the case of solar PV, two semiconductor materials are configured in a positive-negative junction, a p-n junction. The positive and negative properties of the materials are achieved through doping – artificially introducing a charge bias in the two materials. When configured in a p-n junction, a depletion region is formed between the two materials in the junction. This electromagnetic field creates a voltage disparity between the two materials. By connecting the two materials in an electric circuit, electrons will be transported through the circuit in a direct current, performing work while returning to the PN-junction to fill one of the electron “holes” created as another electron gets excited [25]. Figure 6 shows a cross-section of a PV cell.

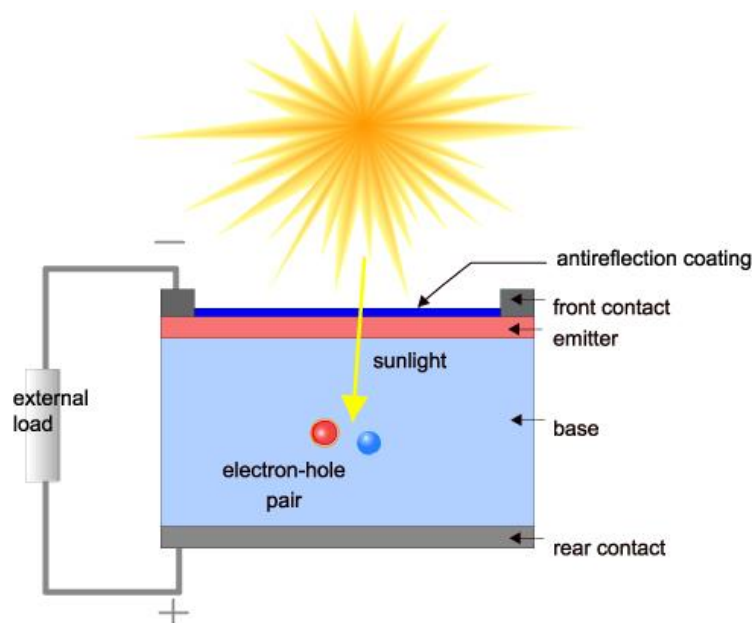


Figure 6: Structure of a solar PV cell. The emitter is negatively doped, while the base is positively doped. The two form a PN-junction. [25]

2.3.2 Solar Radiation

The Sun is the central star of the solar system. Constant nuclear fusion caused by the enormous gravitational forces creates an electromagnetic radiation of immense magnitude. With the surface temperature of the black body of the sun known, Stefan-Boltzmann Law can be used to calculate the magnitude of the electromagnetic radiation. Using the following parameters:

$$\begin{aligned} \text{Radius } R &= 696000000 \text{ m [26],} \\ \text{Surface area } S &= 4\pi R^2 = 6.08 \cdot 10^{18} \text{ m}^2 \text{ [26],} \\ \text{Surface temperature } T &= 5778 \text{ K [26]} \end{aligned}$$

And the Stefan-Boltzmann constant:

$$\sigma = 5.67 \cdot 10^{-8} \text{ Wm}^{-2}\text{K}^{-4} \text{ [28]}$$

The energy radiating from the sun can be calculated:

$$\begin{aligned} E_{sun} &= S \cdot \sigma \cdot T^4 \\ &= 6.08 \cdot 10^{18} \text{ m}^2 \cdot 5.67 \cdot 10^{-8} \text{ Wm}^{-2}\text{K}^{-4} \cdot (5778\text{K})^4 \\ &= 3.84 \cdot 10^{26} \text{ W} \end{aligned}$$

Meaning that the sun radiates 384 Yottajoules per second. The earth being a comfortable 149600000 km, 1 AU, from this nuclear reactor [27], the solar constant at the earth's distance from the sun, G, can be calculated:

$$\begin{aligned} G &= \frac{E_{sun}}{4\pi AU^2} \\ &= \frac{3.84 \cdot 10^{26} \text{ W}}{4\pi \cdot (1.496 \cdot 10^{11}\text{m})^2} \\ &= 1365 \text{ Wm}^{-2} \end{aligned}$$

1365 Wm^{-2} is the solar radiation per square meter on a surface perpendicular to the sun without an atmosphere at the earth's distance from the sun. What this equation does not account for, is the distance that the sunlight must travel through the atmosphere.

2.3.3 Atmospheric Effects

As the electromagnetic radiation travels through the gases of the atmosphere, some of the radiation is absorbed, while some is reflected. This means that the radiation that hits the surface of the earth, is not a perfect spectrum that can be expected from a black body at 5778 K. In figure 7, the atmospheric effects on incoming solar radiation are accounted for. The red line shows the solar spectrum above the atmosphere, which is the 1365 Wm^{-2} discussed previously. The green line shows the spectrum below 1.5 atmospheres, or an angle of incidence of 48.2° . AM is short for Air Mass and is the amount of atmosphere the radiation must travel through. A lower angle of incidence means a higher Air Mass value.

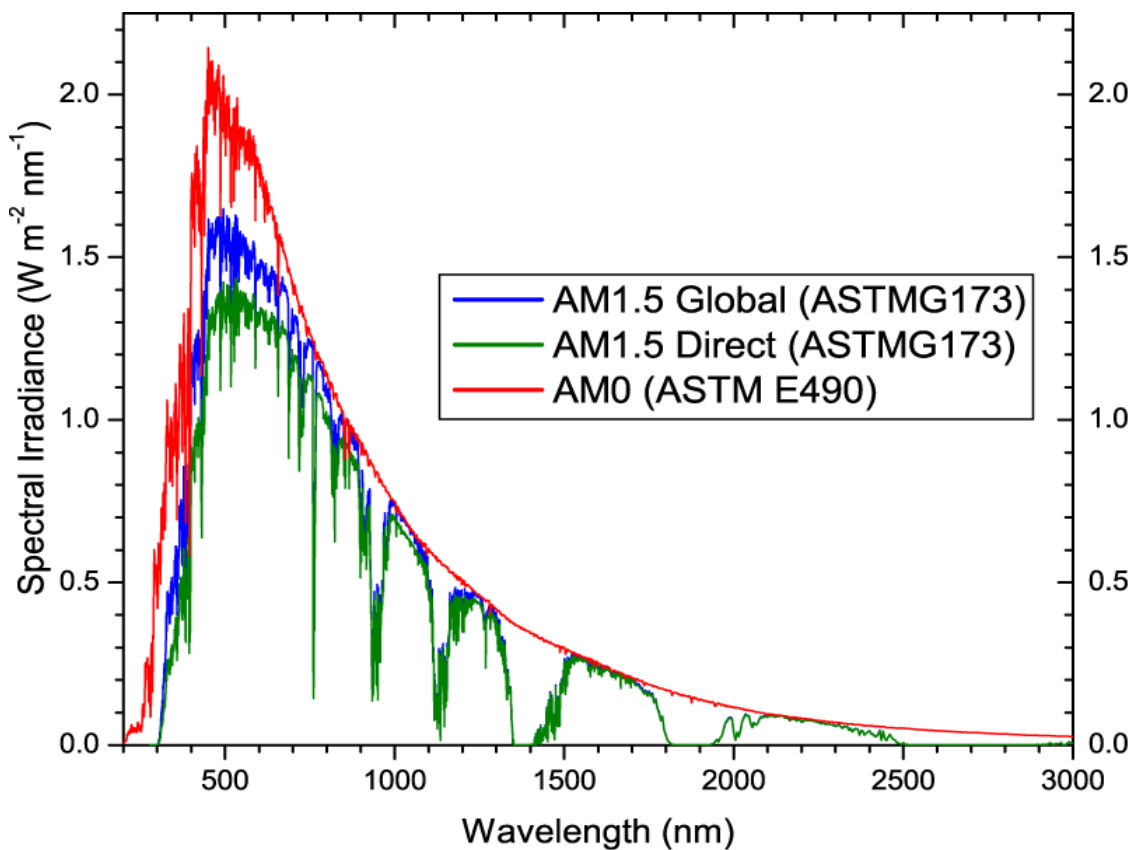


Figure 7: Spectral irradiance for AM 0, AM 1.5 Direct and AM 1.5 GHI [29]

A quick way to approximate the AM value for incoming solar radiation, is to simply divide 1 by the cosine of the angle of incidence, θ , measured from the vertical line [30]:

$$AM = \frac{1}{\cos \theta}$$

This approximation works well for most lower angles but does not account for the curvature of the earth. When the sun gets closer to the horizon, as it often does in the Arctic, the equation gets more complicated [31]:

$$AM = \frac{1}{\cos \theta + 0.50572(96.07995 - \theta)^{-1.6364}}$$

For 90 °, or at the horizon, this yields AM 37.92. The simplified approximation would be dividing by zero for 90 °, and AM approaches infinity as the angle approaches 90 °. Figure 8 illustrates how the approximation works well until approximately 80 degrees, where it quickly deteriorates from the accurate equation for AM.

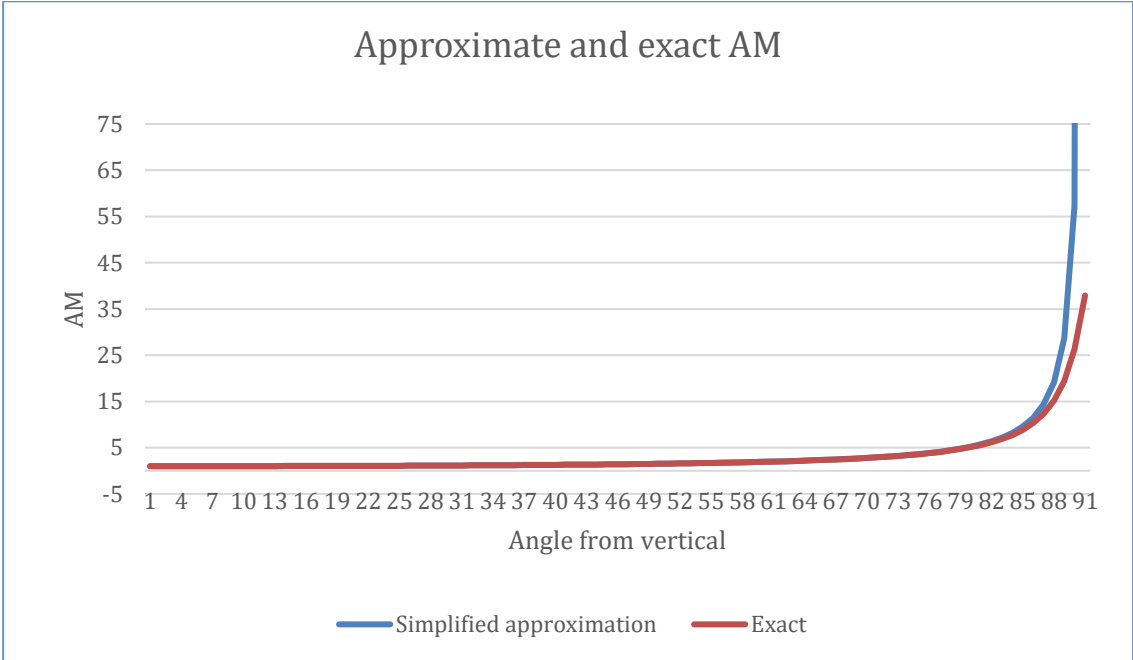


Figure 8: Air Mass with the simplified and exact method

2.3.4 Global Horizontal Irradiance and Albedo

Global Horizontal Irradiance (GHI) is the sum of all radiation that hits a horizontal surface of the earth. This includes reflected radiation from the surface of the earth, diffuse radiation, and the direct radiation from the sun [32]. The blue line in figure 7 represents average GHI with an AM of 1.5. The reflected radiation is highly dependent on the albedo of a surface.

The albedo of a surface describes its ability to reflect radiation as a number between 0 and 1. A surface with an albedo of 1 reflects all radiation, while a surface with an albedo of 0 absorbs all radiation [33]. While soil, forests, and cropland have albedos ranging from 0.10 to 0.35, fresh snow has an albedo of up to 0.90 [33]. This means that 90% of incoming radiation is reflected. The high albedo of snow increases GHI significantly in snowy conditions, suggesting increased potential for solar power production.

2.3.5 Standard Testing Conditions

The standard testing conditions, STC for short, are industry standard testing conditions that most solar PV cells are tested at. The conditions are 25 °C, or approximately 300 K, 1000 W/m² solar spectrum, and Air Mass 1.5 [34]. The rated efficiency of a solar panel is the efficiency under STC. The rated power output of a solar panel is the power output under STC, and is given in W_p , Watt Peak.

2.3.6 Effect of Temperature

The efficiency of silicon PV cells is temperature dependent. High temperatures will lead to a decrease in efficiency, while low temperatures lead to increased efficiency. For silicon cells, the Open Circuit Voltage V_{oc} will decrease by about 0.4-0.5% per °C [35], while the Short Circuit Current I_{sc} will increase slightly by about 0.06% per °C [35]. As the maximum power output is the product of V_{oc} and I_{sc} , the efficiency will decrease as temperature increases. The effect is approximately 0.5% per °C [35].

2.3.7 Bifacial Solar Panels

Bifacial solar panels have technology that allows both sides of the panels to carry out the photovoltaic effect. Panels that have an unobstructed backside will often benefit from bifacial technology, in the form of increased efficiency. This allows the panel to absorb reflected radiation from behind, and also the sun if it passes both in front and behind the panel during a day. Bifacial technology has been proven to be up to 11 % more effective than traditional panels [36].

2.3.8 Solar Tracker Systems

Solar tracker systems are systems that rotate the solar panel, tracking the sun. The idea is to maximize the amount of solar radiation that hits the solar panel. In theory, two axis rotation on a solar panel allows for an optimal angle of incidence, 90° , at all times. Combining tracker systems and bifacial panels, have shown an efficiency increase of up to 27 % [36], compared to non-bifacial static panels.

2.3.9 Global Market

The global market for solar PV has seen exponential growth in the later years, with the Asia Pacific region leading the charge. In 2019, at least 114.9 GW_p of solar PV was installed globally, and the global capacity passed 627 GW_p [37 p. 6], as shown in figure 9. China has been the leading actor for several years, while Germany has the most installed capacity per capita at 595 W_p / capita [37 p. 7].

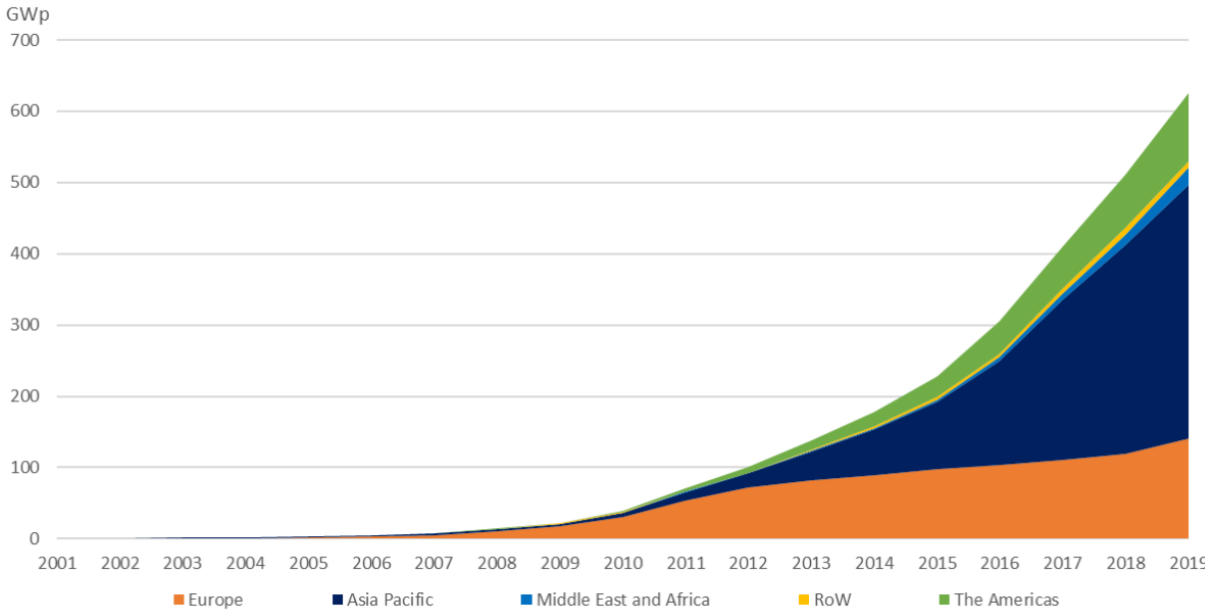


Figure 9: Global solar PV capacity from 2000 to 2019 [37]

2.4 Energy Storage

Energy storage is crucial to provide a stable and reliable energy supply from renewable energy sources. The intermittent nature of many renewable energy sources, like wind and solar, creates a supply which rarely matches the demand. An energy storage system allows surplus energy to be stored in times of over-production, and the stored energy can be depleted in times of production shortage. In stand-alone and off-grid energy systems, like most energy systems in the arctic region, energy storage would be required to provide a reliable energy supply with renewable energy. Additionally, energy storage is useful to limit the changes in load from existing energy systems due to intermittency.

In smaller systems connected to a larger energy grid, a storage unit is not required for providing stable energy unless there is an outage on the grid. It can, however, help reduce the price of electricity for the owner. This can be done by consuming stored energy when the grid electricity is expensive and charge the storage when the grid electricity is cheap.

Several energy storage technologies exist, most of them with drawbacks and advantages. There will always be compromises between storage capacity, discharge time, cost and many more factors. It is important to choose the right storage technology for the system that it will serve.

2.4.1 Round-Trip Efficiency

In all stages of an energy storage process, some of the energy will be lost to the surroundings. The first law of thermodynamics states that energy can never be created, only transform into another form of energy [38]. In every energy conversion process, some energy will be lost to friction, self-discharge, chemical processes, and other loss effects. In energy storage systems with many steps of energy conversion, the term round-trip efficiency is used to express the total energy loss, from the energy is stored until it is being consumed. This figure is the ratio between energy that is put into the system and the useful energy that is available after the storage process.

2.4.2 Batteries

Batteries store energy as electro-chemical potential. There are several battery technologies available, both large and small scale. The high energy density of li-ion technology is valuable for portability, for example in mobile phones and electric vehicles. The energy density of li-ion batteries ranges from 100 to 300 Wh/kg, or 360 to 1080 kW/kg [39]. Expected lifetime can be up to 2000 cycles or more. The round-trip efficiency of li-ion batteries can be over 90%. [40]. Other battery technologies include lead-acid batteries, which has a lower cost than li-ion in exchange for lower energy density.

2.4.3 Heat Storage

Heat storage is an energy storage technique with many technologies [41]. In short, it works by producing heat during energy production surplus, and store it in long-term storage reservoirs. Boreholes are often used to store the energy deep underground. In the Arctic, this introduces many challenges, especially because it interferes with the permafrost that is present in the ground. Thawing of permafrost leads to unpredictable and serious manipulation of the soil. There are, however, potential in the bedrock. Longyearbyen Lokaltstyre is interested in exploring this potential [16].

2.4.4 Compressed Air Energy Storage

Compressed Air Energy Storage (CAES) is an energy storage technology where air is compressed in a sealed container during energy production, and then decompressed through a turbine during energy discharge. The system consists of an energy source, a compressor, a container for pressurized air, a turbine, and the electricity generator (a). Round-trip efficiency for existing plants in Germany is 42% [42 p. 4]. More advanced renditions of the system (b), which stores and make use of the waste heat from the compressor and generator, are estimated to be able to produce efficiencies of 60-80% [43 p. 12-13].

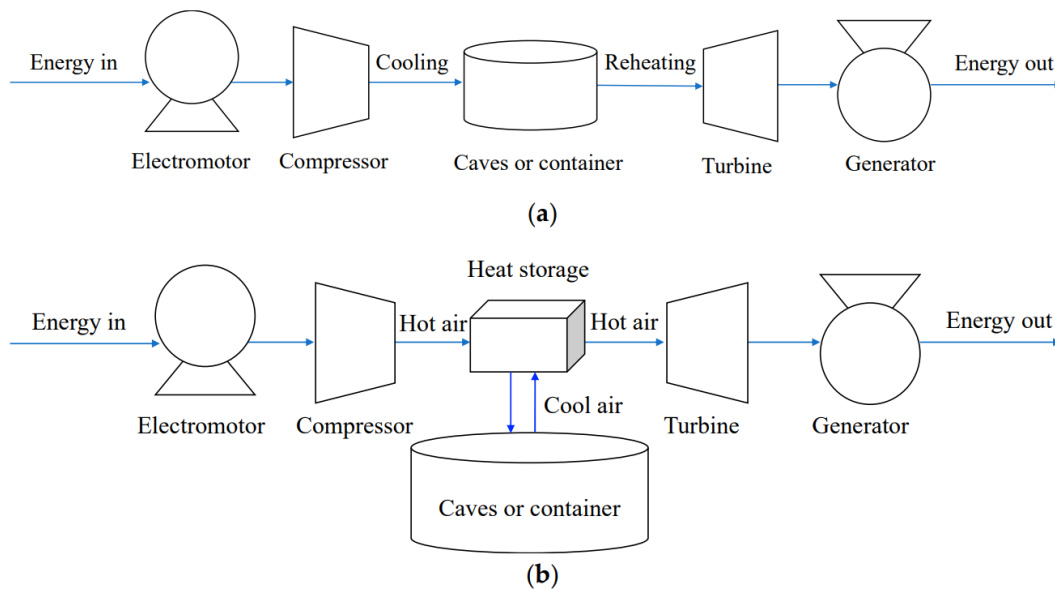


Figure 10: Compressed Air Energy Storage systems, simplified (a) and more efficient with heat storage (b) [42]

One of the challenges with CAES, is the low energy density. Figures range from 2-6 Wh per liter [43 p. 2]. The cause of the low energy density is the high demand for space to store the compressed air. Suggested designs often utilize existing infrastructure, such as abandoned mines. Pilot projects with storage in huge bags at the seabed also exist. The Spitsbergen settlements are in a unique position, where the major settlements were all formed around the coal mining industry. In the record year 2007, around 4.1 million tons of coal were extracted on the island [44 p. 8]. A coal density of 1.5 kg/m^3 [45] will mean that over 2.7 million cubic meters of potential storage volume was created in 2007 alone. Transformed to CAES, that is approximately 5.4 – 16.2 GWh of energy storage.

2.4.5 Hydro and Pumped Hydro Storage

Hydro and pumped hydro storage works by increasing the potential energy of water with surplus energy. In normal hydro dams, this is done by stopping the water flow when the energy is not needed, allowing the reservoir to fill up with rainwater transported there through the natural water cycle. In pumped hydro, pumps are installed to reverse the operation during energy surplus, aiding the natural water cycle.

Hydro and pumped hydro storage are two very efficient storage options. Pumped storage, the least effective of the two because of the reverse operation introducing an extra step of energy loss, sees efficiencies between 70 and 84 % [46 p. 51]. Hydro storage has geographical and climatic limitations. The problem in the Arctic is mainly climatic. Permafrost in the ground means that hydro storage systems are unfeasible because of freezing.

2.5 Capacity Factor

Capacity Factor (CF) is the ratio between net energy production, and theoretical production at maximum capacity in the same time span [47]. It is calculated in a set time span, often a year or a month, and gives an insight on the performance of an energy source. The equation for capacity factor is given as:

$$CF = \frac{P}{P_{max}}$$

Where P is generated energy, and P_{max} is theoretic energy generated at full capacity. For solar PV, the capacity Factor is given as the energy produced over a given time frame, divided by the theoretical maximum production in the same time frame. The maximum production rate is given under STC, and the equation for a given time frame of n days is:

$$CF = \frac{P(n)}{24 \text{ h/day} * n \text{ days} * P_{max}}$$

This is usually done for monthly and yearly figures, giving $n = 28/29/30/31$ depending on month, or 365/366 for yearly figures, and then the produced energy, P(n), for that given time frame.

Capacity factor varies considerably across different energy sources. While nuclear energy can reach as high as 90% [48], most fossil sources hovers around 50 % [48]. Typical values for the renewable sources range from 11 % for the worst performing large scale solar [47], to 40 % for hydro and wind. Some typical capacity factors for different technologies are listed in table 1 [48][50][47].

Table 1: Average capacity factor of some energy sources [48][50][47]

Technology	Location	Average Capacity Factor
Solar PV	Britain	11.7 % [47]
	USA	25 % [50]
	Germany	11.2 % [51 p. 44]
Wind	Britain, offshore	39.6 % [47]
	Britain, onshore	26.2 % [47]
	USA	34 % [50]
Nuclear	USA	92.6 % [48]
Hydro	USA	40 % [48]
Coal	USA	54 % [48]
Natural Gas, CC	USA	57 % [48]

Calculating capacity factor the renewable energy sources is often more valuable than for the fossil sources. For fossil energy, capacity factor is not location specific, and since the energy resource is readily available, capacity factor mostly says something about what efficiency and load the power plants operate at. For renewables, capacity factor says more about the availability of the energy source and how well the resource is being utilized. In solar PV, 100% capacity factor would occur if the solar cells operated under STC at all time.

3 Method

3.1 Svalbard Airport Solar Facility

Situated at 78 degrees, 14 minutes, and 46 seconds north, is Svalbard Airport, Longyear. It operates daily flights to and from mainland Norway and is the world’s northernmost commercial airport. Avinor is responsible for the operations at the airport [52].

Avinor has a goal of halving their total CO2 emissions from operations from 2012 until 2022 [53]. Svalbard airport, in particular, has been targeted by Avinor to meet this goal [54 p. 35], stating that:

“Svalbard Airport in particular stands out in Avinor’s climate accounts as the airport’s heating and electricity are both provided by a coal-fired power plant.” [54 p. 35]

In their own calculations, Svalbard Airport is third on the list over sources of greenhouse gas emissions, producing more than 2000 tons of CO₂ equivalents annually, as illustrated in figure 11. Looking to reduce the produced CO₂ equivalents at Svalbard Airport is therefore a reasonable measure to meet that target.

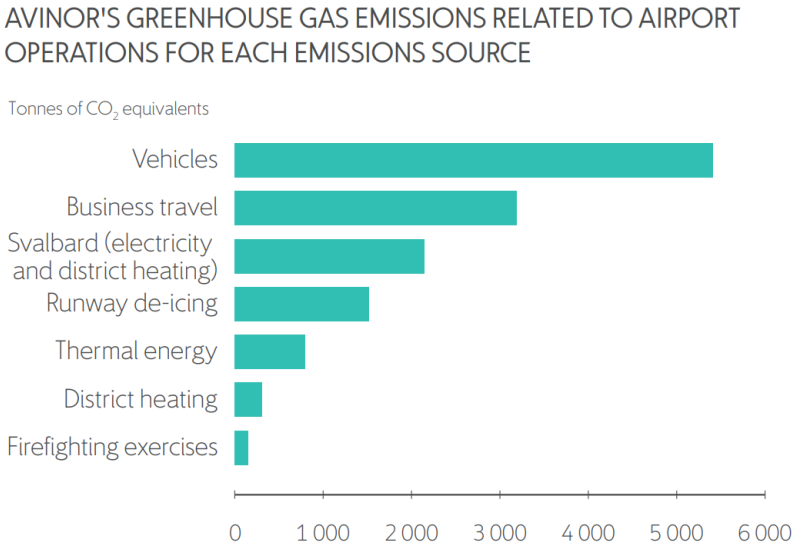


Figure 11: Avinor’s Greenhouse Gas Emissions Related To Airport Operations For Each Emission Source [54]

3.1.1 Sun Conditions

Svalbard Airport is around half-way between the North Pole and the Arctic Circle, and experiences both the polar winter and the midnight sun. From October 26th to February 15th, the sun is below the horizon throughout the day, and from April 19th to August 23rd, the sun will not set [55]. In addition, the sun does not rise very high above the horizon, peaking at 35 ° above the horizon at mid-day on summer solstice, June 21st [56].

The Airport is situated directly north of the Platåfjellet plateau, which obstructs parts of the incoming solar radiation (figure 12). At a distance of 1.8 km from the airport, and an elevation of 450 meters above sea level, the angle created towards the airport is around 14 ° from the horizontal. This reduces the available solar radiation by quite a bit. Illustrated in figure 12, is the path of the sun at summer solstice (upper path), and spring/autumn equinox (lower path). It is noticeable that Platåfjellet interferes with the sun at the equinoxes. However, between March 28th and September 15th, the Platåfjellet does not interfere with the incoming solar radiation from south [57], as the sun's path is higher than the plateau.

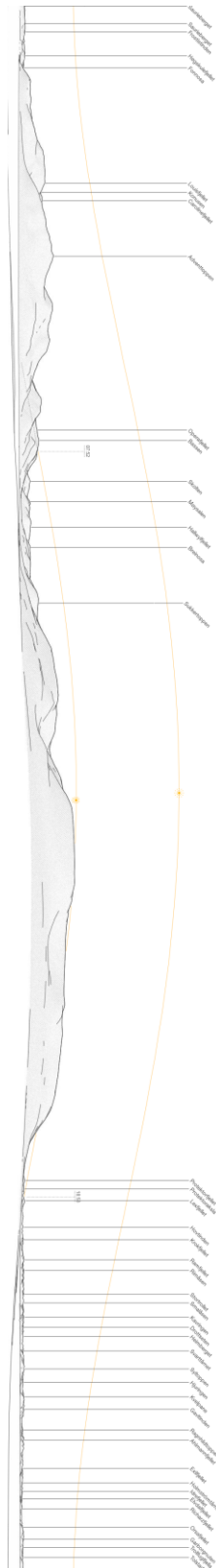


Figure 12: 360 degree horizon as seen from Svalbard Airport. Included are the sun's path at summer solstice, and spring and autumn equinox. Winter solstice is below the horizon [57]

3.1.2 Weather

The historic weather data from Longyearbyen Airport is very detailed, due to a weather station at the airport. It has been operational since 1980 [58]. Most relevant for solar PV production, is data on cloud cover, temperature, and precipitation. Figure 13 shows an average cloud coverage throughout the year. It is observed that the months between April and October sees a higher chance of clearer skies, while the months from November to December have as high as 70% chance of being overcast. Fortunately for solar PV, that means that the highest chance of overcast, happens when the sun is below the horizon.

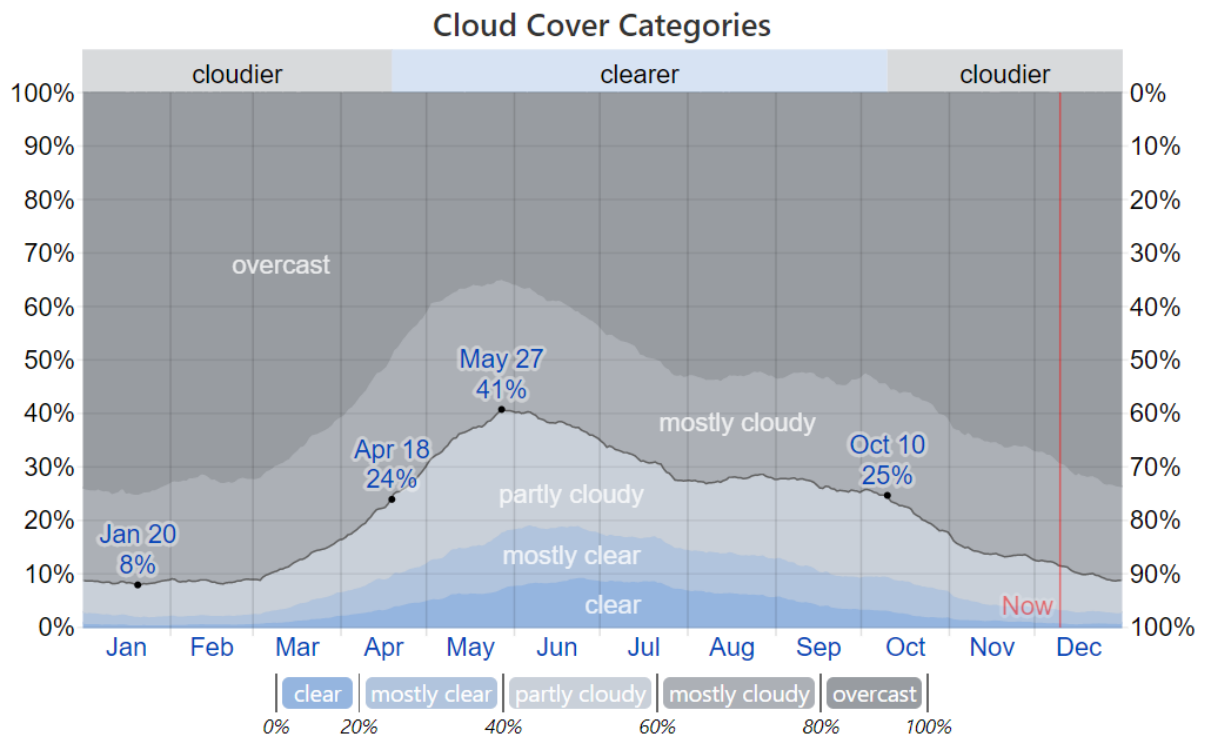


Figure 13: Average cloud cover at Svalbard Airport since 1980 [58]

Average temperature in the winter months is between -6 and -16 °C [58]. The red line in figure 14 shows the highest average temperature, while the blue shows the lowest. Temperatures can drop towards -30 °C in winter. Summer temperatures rarely exceed 15 °C, but in 2020 a new temperature record was set. July 25th, the temperature at Svalbard Airport reached 21.7 °C, the highest ever recorded on Spitsbergen [59].

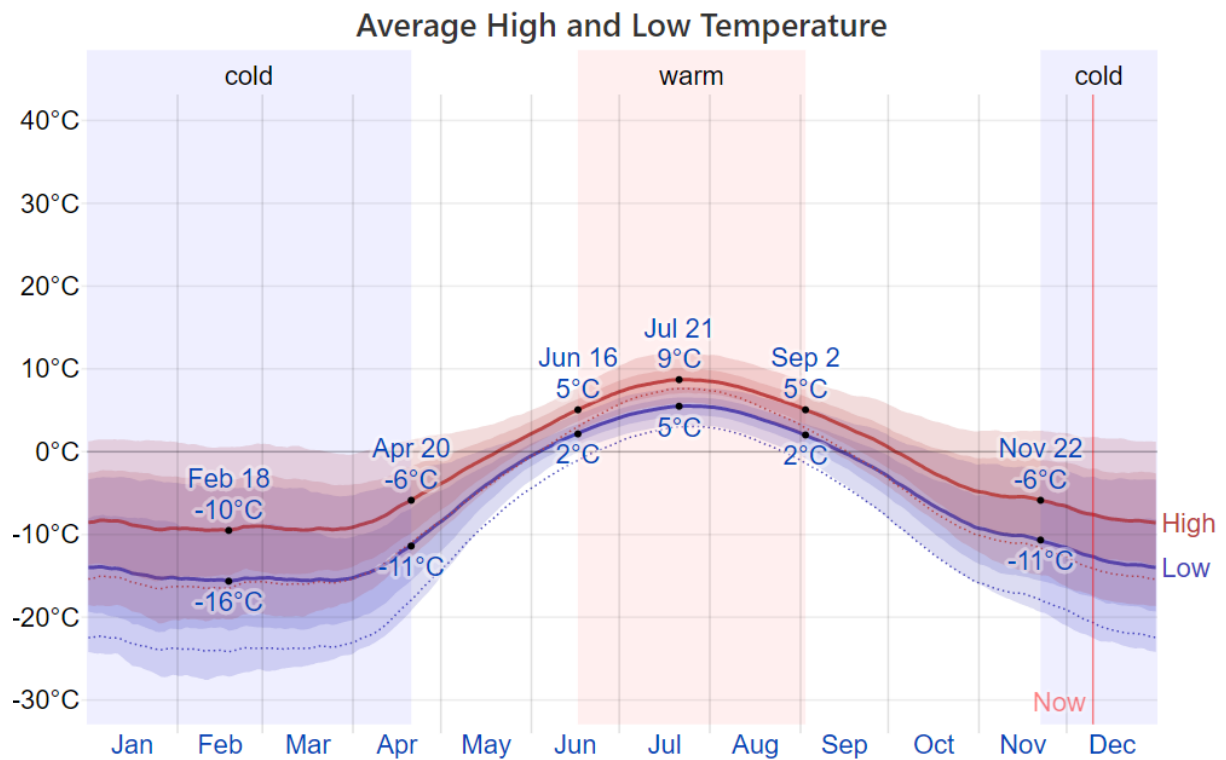


Figure 14: Highest and Lowest Average Temperatures at Svalbard Airport since 1980.

The later years have seen a drastic increase in temperature and precipitation in Longyearbyen, contributed to the ongoing climate change [4]. Historic data might therefore not reflect the future weather in the best way. It is, however, an indicator that is valuable if used with caution.

3.1.3 Solar Panels

As part of the goal to halve the CO₂ emissions by 2022, Avinor began installation of a Solar PV system on Svalbard Airport in 2016. It was initially a pilot project, but it performed better than expected due to reflection [60 p. 41]. It was therefore decided to expand the facility in 2017, and it was further expanded in 2018. It now consists of 450 PV modules, 32 of which are roof mounted, and 418 wall mounted [61 p. 15-16]. Since installation of the latest modules in 2018, it has produced at full capacity for the entirety of 2019 and 2020.

The solar PV installation on Svalbard Airport consists of a mix of two brands of solar panels, with varying specifications. There are 150 Jinko JKM265P and 300 Sunpower E20-327

panels [61 p. 15-16]. The key characteristics of each of the panels are listed in table 2. Most notable is the different cell type, mono- and polycrystalline. Monocrystalline is known to have a higher efficiency than polycrystalline, as they are created from a single silicone crystal. Consequently, the price is also higher [62].

Table 2: Specifications of the solar PV panels installed at Svalbard Airport

	Sunpower E20-327 [63]	Jinko JKM265P [64]
Cell type	Mono Crystalline	Poly Crystalline
No. of cells	96	60
Avg. efficiency	20.4 %	16.19 %
Peak Power	327 W _p	265 W _p
Degradation (Warranty)	5% first 5 years, 0.4% annual next 20	2.5% first year, 0.7% annual next 24
Temperature coeff., P _{max}	-0.35 % / °C	-0.41 % / °C

The total installed PV capacity of Svalbard Airport as of December 2020 is:

$$kW_p = 300 \cdot 327 W_p + 150 \cdot 265 W_p = 137.9 kW_p$$

3.1.4 Degradation

The two types of panels on Longyearbyen Airport are rated with a degradation rate of 5% for the first 5 years, then 0.4% annually for the monocrystalline Sunpower E20-327 [63]. The Jinko JKM265P has a degradation rate of 2.5% the first year, then 0.7% annually after that [64]. Illustrated in figure 15, the monocrystalline panels generally have a lower degradation except for after 5 years, where it for a short time has a higher degradation than the

polycrystalline panel. It must be noted that these degradation rates are worst case, as the provider guarantees higher efficiency than the rated degradation.

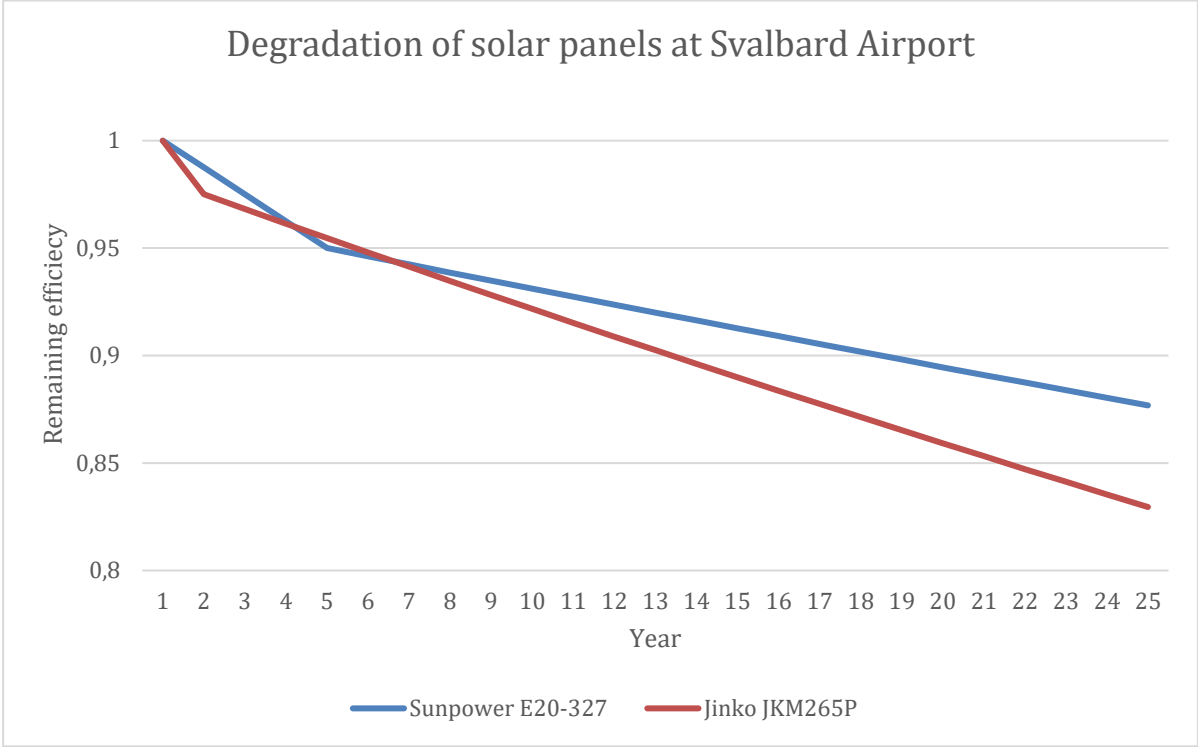


Figure 15: Expected degradation of the solar PV panels at Svalbard Airport

3.1.5 Inverters

There are 11 inverters that convert the direct current generated by the solar panels to alternating current that can be consumed by the power grid. They are all Fronius Symo inverters, with varying capacities. The Fronius Symo inverters are delivered in 15 configurations from 3 kW to 20 kW [65]. In the Svalbard Airport facility, there are four 10 kW, two 12.5 kW, two 15 kW and three 20 kW inverters [61 p. 16-17], totaling a maximum capacity of 155 kW. They have the following panels connected to them:

Table 3: Inverters at Svalbard Airport and the connected solar panel arrays, Panel configuration and installation year

Inverter capacity [kW]	Panel model	Panel amount	Total capacity [kW _p]	Panel orientation	Panel tilt	Installation year
10	Jinko JKM265P	20	5.3	15 °south/west	Vertical	2018
10	Jinko JKM265P	25	6.26	15 °south/west	Vertical	2018
10	Jinko JKM265P	25	6.26	15 °south/west	Vertical	2018
10	Sunpower E20-327	24	7.85	15 °south/west	Vertical	2018
12.5	Sunpower E20-327	40	13.08	15 °south/west	Vertical	2017
12.5	Sunpower E20-327	40	13.08	15 °south/west	Vertical	2017
15	Sunpower E20-327	40	13.08	105 °west/north	Vertical	2018
15	Sunpower E20-327	40	13.08	105 ° west/north	Vertical	2018
20	Sunpower E20-327	24, 16, 16 (56 total)	18.31	15 °south/west, -75 ° east/south, 105 ° west/north	15 ° from horizon, Vertical, Vertical	2016
20	Jinko JKM265P	80	21.20	15 °south/west	Vertical	2017
20	Sunpower E20-327	60	19.62	15 °south/west	Vertical	2018

3.1.6 Orientation of Panels

The panels are placed on the buildings of the terminal, the control tower, and hangars. Most of the panels are mounted on the south-west facing wall, but some are roof mounted and mounted on a west-north facing wall.

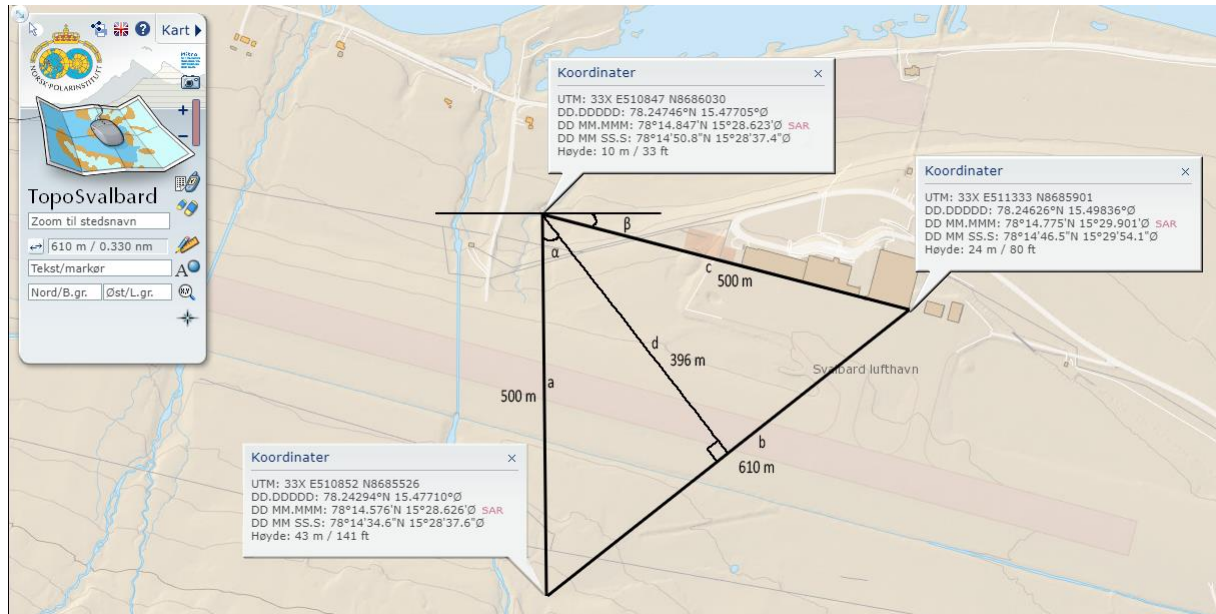


Figure 16: Calculation of the orientation of wall mounted solar panels [13]

To find the direction of the panels, the detailed Svalbard map from Norsk Polarinstittutt [13] was used. Referencing figure 16, the method was as follows: Line c was drawn 500 meters parallel to the south-west facing walls of the airport. From the end of c, line a was drawn in longitudinal direction, also 500 meters. Lastly, line a was drawn from the end of a back to the beginning of c, measured to 610 meters long. Basic trigonometry can be applied to find the angles. The Pythagorean Theorem finds the length of d:

$$\left(\frac{b}{2}\right)^2 + d^2 = a^2$$

$$d = \sqrt{a^2 - \left(\frac{b}{2}\right)^2} = \sqrt{500^2 - \left(\frac{610}{2}\right)^2} = 396 \text{ m}$$

Knowing the lengths of all the sides in a right triangle, any of the three trigonometric functions can be used to find an angle. To find α , the cosine function was used:

$$\cos(\alpha) = \frac{d}{a}$$

$$\alpha = \cos^{-1}\left(\frac{d}{a}\right) = \cos^{-1}\left(\frac{396}{500}\right) = 37.6^\circ$$

Ultimately, the angle β is the one that is interesting, as it is the angle that the south walls of the airport buildings differ from the latitudinal parallel:

$$\beta = 90^\circ - 2\alpha = 90^\circ - 75.25^\circ = 14.75^\circ$$

This means that the south-west walls of the airport are facing 15° south-west from the latitudinal parallel. This differs slightly from the 20° stated by Enoksen [61 p. 15-16].

3.1.7 Production Data

The production data from the facility at Svalbard Airport is available for the system administrators through the Fronius International owned “Solarweb”. In addition, guests can be granted viewing access from the administrator. For the current project, permission for data insight was granted by the previous airport manager, Carl Einar Ianssen.

Each of the 11 inverters provides detailed production data, with a sampling interval of 5 minutes. This data is converted to daily, monthly, and yearly production figures. More specific data, like current and voltage, are also available. Daily power production from every one of the 11 inverters is what will be used as the data base of this thesis.

From the 11 inverters, a daily energy production is logged on Solarweb. That means that yearly, over 4000 data entries are logged. Without a download option, or the capability to automate the data logging, each entry had to be manually logged for data processing. The work is tedious, and prone to mistakes. After careful review, and matching the monthly totals for each channel with the monthly totals of Solarweb, the confidence in the accuracy of the manually recorded values is high. No transcription mistakes were found in the final, careful, review.

The daily production data for every channel, is plotted in figure 17. The name of the channels in the legend are the same as they are on Solarweb. All production from the different channels is stacked, so the total daily production of the system is illustrated. It is easy to see the two expansions, in the beginning of 2017 and towards the end of 2018. The best production days after the last expansion in 2018 is shown to be over 900 kWh. The seasonal behavior of the solar resource is clearly demonstrated, also the huge day-to-day variation in production during the summer season.

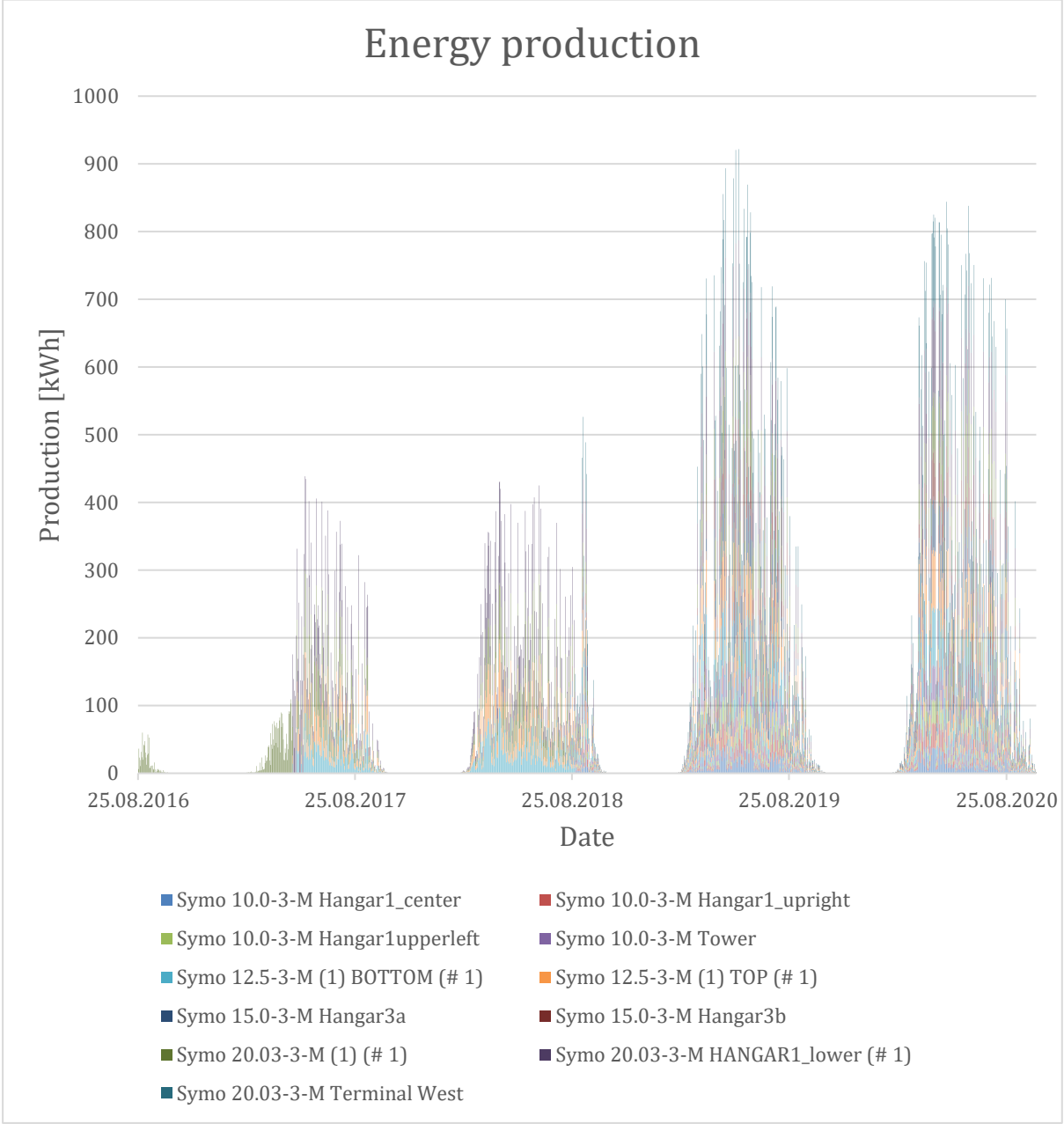


Figure 17: Energy production for each of the 11 arrays at Svalbard Airport.

The channels in Solarweb are not intuitively named and lack consistency. It therefore required some work to identify what channels relate to what solar panel array. The names of the channels start with what size inverter it is connected to. For example, the “Symo 10.0-3-M Hangar1_center” is connected to a Fronius Symo 10 kW inverter. Then, using what year they started producing, combined with Enoksen’s previous work [61 p. 15-17], specific identification could commence. Five of the channels are identified in figure 18, all wall mounted and facing 15 ° south-west. “Symo 15.0-3-M Hangar 3a” and Symo “15.0-3-M Hangar3b” are the two arrays that are wall-mounted in a 105 ° northwestern direction. “Symo 12.5-3-M (1) BOTTOM (# 1)”, “SYMO 12.5-3-M (1) TOP(# 1)” and “Symo 20.03-3-M Terminal West” are all wall mounted on the terminal, 15 ° south-west. In relation to figure 18, they start at the left ending of the figure. Lastly, “Symo 20.03-3-M (1) (# 1)” is the pilot installation, with 32 panels roof mounted, and 24 panels wall mounted. The roof-mounted panels are mounted on the terminal building in an A-shape, with 15 ° inclination. They face 110 ° north-west and -70 ° east-south. The last 24 panels are mounted on the 15 ° south-western wall.



Figure 18: Location of five of the arrays that track production data

3.2 Previous Work

As a baseline for the thesis, existing literature was utilized to gather data and information. The literature is a mix between academic research and private reports conducted by request from the administrating organs of the settlements. What separates this thesis from the reports that are used as baseline, is that actual production data from an arctic PV installation is used in this thesis. The reports from Multiconsult for Longyearbyen [19] and Ny-Ålesund [22], both rely on weather data to estimate PV production. Enoksen's Master Thesis [61] from earlier in 2020 provided great insight in the PV system at Svalbard Airport, and clarified the provided production data from the airport.

3.3 Simulation

To investigate how a solar PV power plant can facilitate an arctic settlement in the future, simulations will be conducted to examine what system sizes are required for different scenarios. Energy consumption data from Multiconsult [19] will be paired with estimated production data, calculated based on the production data from the existing solar PV power plant in Longyearbyen. Storage technology will be included to simulate performances of full-scale system designs.

3.4 Analysis Tool

The initial plan was to use the programming language Python to analyze the data. Python is a relatively intuitive programming language and is great for mathematical operations on lists and other data structures. After discovering that the data from Solarweb was not available for download, a natural choice to use Excel for data entry was made. While copying over 16000 data entries to Excel, a fluid transition to also perform the data manipulation in Excel occurred. Excel is great for visualization of the datasets, and the visual and intuitive handling of data that Excel provides was valued over the, in many ways, more advanced Python. In addition, the mathematical operations and visualization of the results of the analysis did not require the flexibility and computing power that Python provides. The decision was therefore made to use Excel for analysis of the data, scrapping the original plan of using Python.

4 Findings

4.1 Performance of PV in the Arctic

The solar PV facility at Svalbard Airport has been operating at full capacity for the entirety of 2019 and 2020, after the last new expansion was made towards the end of 2018. Two years of data from an installation with a minimum lifetime of 25 years will unfortunately not provide a full representation of the expected yearly energy production. It will, however, provide a valuable indication of what can be expected for future installations in the polar regions, especially if climate and latitude is similar.

4.1.1 Capacity Factor

In 2019, the solar installation in Longyearbyen produced 68.25 MWh, and 67.05 MWh in 2020. The average comes out to be 67.65 MWh. This value inserted to the equation from section 2.5 calculates the average capacity factor for the last two years:

$$CF = \frac{67\,650\,000\text{ Wh}}{365\text{ d} \cdot 24\text{ h/d} \cdot 137\,900\text{ W}} = 0.0560 = 5.60\%$$

A capacity factor of 5.60 % is in the lower end for a solar PV facility, considering that facilities are observed to reach capacity factors of up to 20% as discussed in section 2.5. Knowing that the solar resource is only available in the summer season, it is expected that the capacity factor will vary a lot throughout the year. The 128 days from October 15th to March 20th are without any production at all. Removing these from the annual capacity factor calculation:

$$CF_{production} = \frac{67\,650\,000\text{ Wh}}{(365 - 128)\text{ d} \cdot 24\text{ h/d} \cdot 137\,900\text{ W}} = 0.0860 = 8.60\%$$

A capacity factor of 8.6 % is found for the days with energy production. This is almost comparable with numbers seen in Germany and UK, where the CF hovers around 11%.

To visualize the seasonal variation in solar PV performance, it is helpful to plot the monthly capacity factor to see what role this variation in insolation plays. Monthly capacity factor was found by using the same equation as above, replacing the total energy with monthly energy, E_{month} , and the days with number of days in the month, d_{month} :

$$CF_{monthly} = \frac{E_{month}}{(d_{month}) * 24h/d * 137900W}$$

In figure 19, the calculated monthly capacity factor in 2019 and 2020 is plotted. As expected, October to February has virtually zero production, and all the production happens in the months from March to September. The best performing months are April through August. Monthly capacity factor is seen to peak at over 16%, a very competitive value, beating German and British averages as seen in table 1.

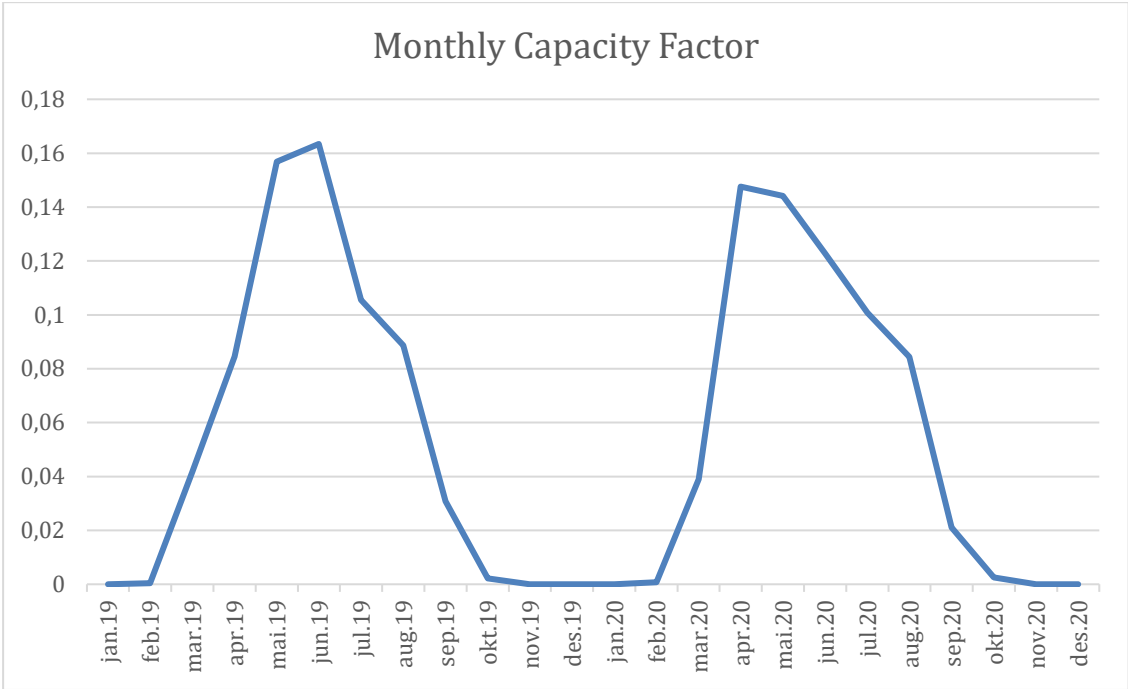


Figure 19: Average monthly capacity factor for the 11 arrays in 2019 and 2020

It is interesting to observe that there seems to be a bias towards better production in the first production months of the year. Several factors can play a role in this, for example better weather in the spring, as seen in section 3.1.2. It is also in line with theory, considering the increased efficiency at lower temperatures, and increased albedo because of the snow cover, that is experienced in the spring months.

When the monthly capacity factor from each of the 11 arrays of solar panels connected to the 11 inverters are plotted, a similar, but more detailed outlook is given. Individual data from each of the arrays provides valuable information for the different configurations. It is surprising that the three different installment configurations at the airport performs similarly.

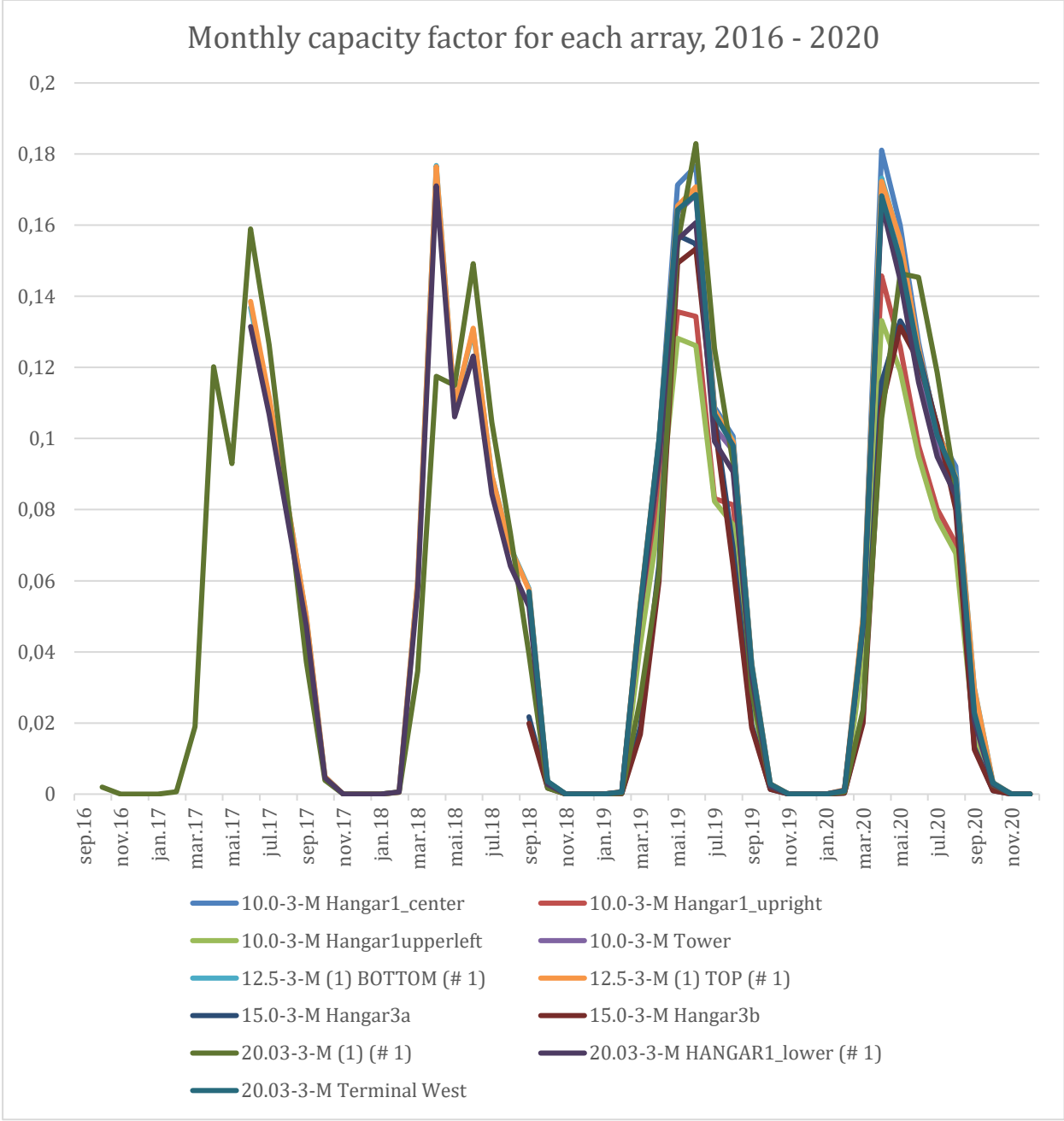


Figure 20: Monthly capacity factor for each of the arrays

The most notable outliers are “10.0-3-M Hangar1_upperleft” and “10.0-3-M Hangar1_upright”. They are observed to perform considerably worse than the rest of the arrays. Initially, it was assumed that this was caused by poor selection of inverter. However, Fronius states that the 10 kW inverters only will have a drop off in adaptation efficiency of around 5% when the scaling is in the magnitude of the system in question [65]. Additionally, “10.0-3-M Hangar1_center” is one of the best performing arrays when it comes to capacity factor, while filling even less of the inverter’s capacity.

A suspicion of what the cause of the bad performance of the two arrays arose as pictures of the facility were carefully studied. An extension of the wall of the hangar, which the center array is placed on, creates a shadow on the western array, “10.0-3-M Hangar1_upperleft” in the morning, and eastern array, “10.0-3-M Hangar1_upright” in the evening. In figure 18, the source of this shadow is the part of the building where “10.0-3-M Hangar1_center” is installed.

The suspicion was confirmed when analyzing the daily production data from the arrays. The two arrays have a symmetric, but shifted, pattern, where the eastern panels have their peak approximately 1h20m before the western panels have their peak. In figure 21, this effect is shown. April 8th, 2020 was clearly a day of high production. In the morning, the “10.0-3-M Hangar1_upperleft” is shaded while “10.0-3-M Hangar1_upright” produces at full capacity. After mid-day, it shifts, and “10.0-3-M Hangar1_upperleft” produces more than “10.0-3-M Hangar1_upright”. For some reason, the legend in Solarweb is wrong. “10.0-3-M Hangar1_upright” and “10.0-3-M Hangar1_upperleft” have the same installed capacity, 6.26 kW, while the center installation has 5.3 kW. This can be confirmed by counting the panels in figure 18. The legend in figure 21 should be swapped between “Symo 10.0-3-M Hangar1_upperleft” and “Symo 10.0-3-M Hangar1_center”. This is corrected in the rest of the project.

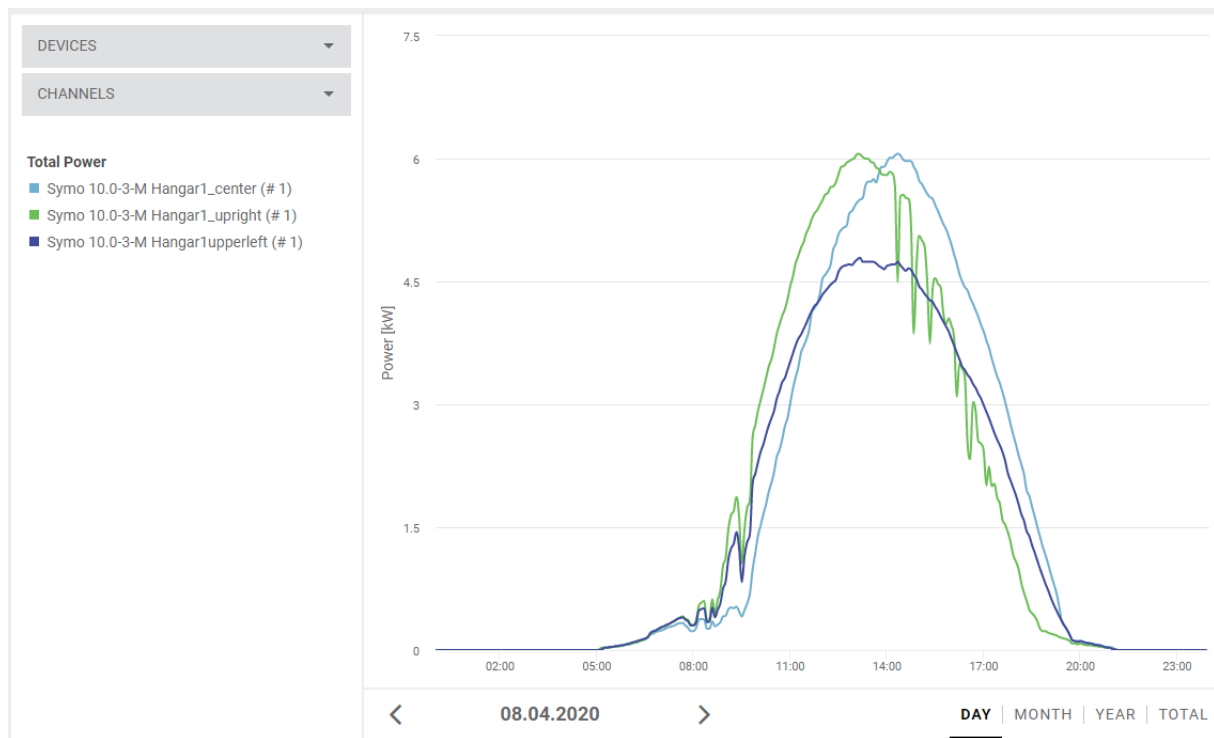


Figure 21: Demonstrating the shifted symmetry of the “10.0-3-M Hangar1_upperleft” and “10.0-3-M Hangar1_upright” arrays, compared to the “10.0-3-M Hangar1_center” array. Legend is wrong from the provider, and corrected in thesis

Peak daily capacity factor from the panels of the airport was also found. Figure 21 shows that the roof-mounted panels have a lower peak CF than the rest of the panels. Additionally, the two shaded panels are experiencing low maximum CF. Meanwhile, the panels on the part of the building that shades these panels have the highest peak CF. The panels that are shaded have their capacity factor reduced by up to 25% on peak days, compared to the center array between the two. The fact that the eastern array of the two shaded arrays have a higher peak CF than the western, might indicate that the early morning production potential is higher than in the evening, because the two installations are perfectly symmetric (figure 18). Maximum capacity factor seems to be in the same range for both the panel brands, and both the south-western and west-northern orientation.

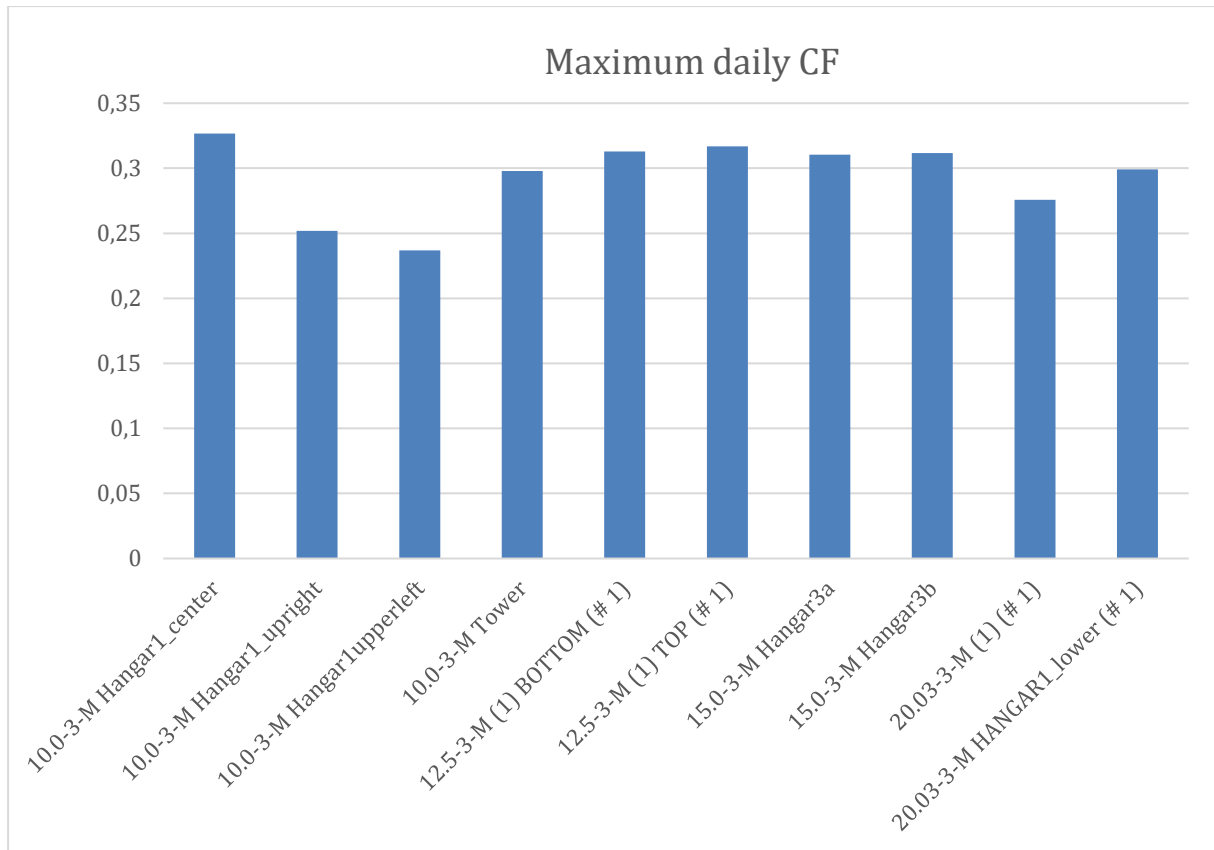


Figure 22: Maximum daily capacity factor since installation for all 11 arrays

4.1.2 Optimal Installation Configuration

With only three different installation orientations, it is challenging to decide a perfect installation configuration. What is possible, is to find out which of the existing configurations performs best. To find an answer to this, three arrays with identical panels and similar size in the three directions were compared. The Sunpower E20-327 panel is installed in all three configurations. Performance of the three panels can be seen in table 2.

Table 2: Capacity factor of three different panel configurations

	12.5-3-M (1) TOP (# 1)	15.0-3-M Hangar3a (# 1)	20.0-3-M (1) (# 1)
Number of panels	40	40	56
Pmax [kW _p]	13.08	13.08	18.31
Inverter size [kW]	12.5	15	20
Installation config.	Vertical, 15 ° south-west	Vertical, 105 ° west-north	Roof-mounted and vertical 15 ° south-west
Capacity factor	6.03%	4.97 %	5.56 %

South-western oriented panels are expected to have a higher capacity factor, than the west-northern oriented. This is in line with expectations. The difference is, however, not very big. A theory for why this is the case, is that during the 360 ° sun from April 20th to August 23rd, daily hours of insolation is unaffected by the orientation of the panel. In a 90 ° orientation to the horizon, west-northern panels are even expected to perform better under these conditions, as the sun will be lower on the sky in the evening. The effect is also reflected in the peak daily CF, shown in figure 22, where the peak CF of the two arrays of northwestern facing panels “Symo 15.0-3-M Hangar 3a” and Symo “15.0-3-M Hangar3b”, are at the same level as the unshaded 15 ° south-west oriented. This can be exploited in areas where weather varies a lot from hour to hour because of local effects. If the evenings tend to have more cloud cover, maybe a more eastern orientation of the panels is advantageous. In addition, it can be useful to avoid shading from surrounding mountains in the same way. For Svalbard Airport, with the Platåfjellet directly to the south (figure 12), the 15 ° south-western orientation is probably not optimal because of shading from the plateau.

A similar comparison between mono-crystalline and poly-crystalline panels was also made. Some of the 2017 installations were chosen for this assessment. They are all wall mounted, facing 15 ° south-west. The three-year average capacity factor was calculated and can be seen in table 3. This might indicate that monocrystalline solar cells will have a higher capacity factor than polycrystalline. However, monocrystalline panels are more expensive, and cost-effectiveness must be considered when choosing cell-technology for a system.

Table 3: Capacity factor of monocrystalline and polycrystalline panels

	12.5-3-M (1) TOP (# 1)	12.5-3-M (1) BOTTOM (# 1)	20.0-3-M HANGAR1_lower (# 1)
Number of panels	40	40	80
Pmax [kW _p]	13.08	13.08	21.2
Inverter size [kW]	12.5	12.5	20
Installation config.	Vertical, 15 ° south-west	Vertical, 15 ° south-west	Vertical, 15 ° south-west
Cell type	Mono	Mono	Poly
Capacity factor	6.03 %	6.03 %	5.65 %

4.2 Improvement Suggestions

There are several ways to improve a new solar PV installation in the arctic region. Enoksen [61] estimated a potential efficiency gain of almost 10% at the airport in Svalbard. The most important contributor to solar PV is the sun. To maximize the efficiency of solar PV it is therefore crucial to maximize incoming solar radiation on the installed panels. The static, 90 °, wall-mounted panels, while simple to install and maintain, have lots of room for improvements.

4.2.1 Tilt

The tilt of most of the panels in the Svalbard Airport PV system is 90 ° from the horizon, perpendicular to the horizon. As the sun spends all its visible hours above the horizon, it is obvious that even the slightest tilt would increase efficiency. A simplified suggestion that would increase annual incoming radiation, is to tilt the panels to the angle in between the horizon, and the highest angle of the sun at summer solstice. This would, in Longyearbyen's case, be:

$$\angle Tilt = 90^\circ - \frac{\angle Horizon + \angle Sun_{solstice}}{2} = 90^\circ - \frac{0^\circ + (90^\circ - 78^\circ) + 23.4^\circ}{2} = 72.3^\circ$$

This would, compared to the 90 ° panels, increase the efficiency of the installed solar panels any time the sun is 9 ° or above on the horizon. Keeping in mind the increased horizon angle from Platåfjellet just south of the airport would further increase the benefits of this tilt. More sophisticated methods can be used to find the perfect angle of tilt in relation to the direction of the panel. It would also be useful to include local weather conditions and shading in the calculations. AM value also increases rapidly at angles closer to 90 ° and must be considered.

One big benefit that vertical tilted solar panels have in the Arctic, is that they are less susceptible to snow cover. Snow cover on solar panels is a known challenge in areas where snow occurs. This is also experienced at Svalbard Airport, where the roof-mounted solar panels with a tilt of 15 ° to the horizon experience efficiency losses after snow fall [61 p. 48]. Tilting the panels introduces snow cover challenges to the system.

4.2.2 Bifacial Technology

To further utilize the high reflection rates from the snow in the polar regions, bifacial solar panels is a promising option. They will benefit both from the 24-hour sun, as well as the ground reflected solar insolation, especially when reflected from snow. Wall mounted bifacial panels will, as expected, not benefit a lot of being bifacial. Because no radiation, neither reflected or direct, will hit the backside of the panel, rendering the bifacial technology useless. This is confirmed in practice, with wall-mounted bifacial panels in Tromsø [61 p. 57]. With a clear backside, simulations show that the efficiency of bifacial modules are more beneficial in an arctic climate compared to a Munich climate [61 p. III].

4.2.3 Tracking Systems

Some of the biggest potential production losses in the Arctic, comes from the static nature of the installed panels. While wall-mounting is very simple and low maintenance, the advantages of the midnight sun are almost completely lost. The exception being some reflected light from the surroundings.

The high latitudes, like the Arctic and Antarctic, will see the highest gains in efficiency when installing two-axis tracker systems [66]. Simulations with two-axis tracking in Narvik, at 68 ° north, shows that the efficiency can increase by 40-45 %, and the increase is most prominent in the summer months [66]. With the variation of angle of the sun decreasing the further from equator one is, the need for two-axis tracking decreases. A single axis tracking system, with static tilt, reduces the complexity of the system, while gaining more hours of production.

Being in the Arctic climate, tracking systems will be high maintenance, because of snow and ice. However, if a stand-alone solar PV system was to be designed, it certainly must be explored. An additional challenge introduced by rotating panels is the shading, and spacing between the installations must be increased to maintain high production.

4.3 Simulation of Solar PV Systems

Using the production data from Longyearbyen Airport, it has been possible to simulate a couple of scenarios of varying degree of solar dependency. With weather being such an important factor in solar energy, data from Longyearbyen is mostly relevant in the Svalbard area. However, most of the other factors are common for the arctic region and can therefore be translated to other locations.

4.3.1 Energy Profile

In a year-round arctic settlement, the energy consumption varies significantly with season. Multiconsult conducted a survey in Longyearbyen in 2018 [19] which found that 40 000 MWh of electricity and 70 000 MWh of district heating were consumed annually by the 1850 customers on the grid [19 p. 13]. The maximum and minimum daily load of district heating and electricity for the year of 2018 are illustrated in figures 23 and 24. It can be observed that

the production of district heating almost doubles in the winter season. Electricity consumption also increases in the winter, but not nearly with the same magnitude.

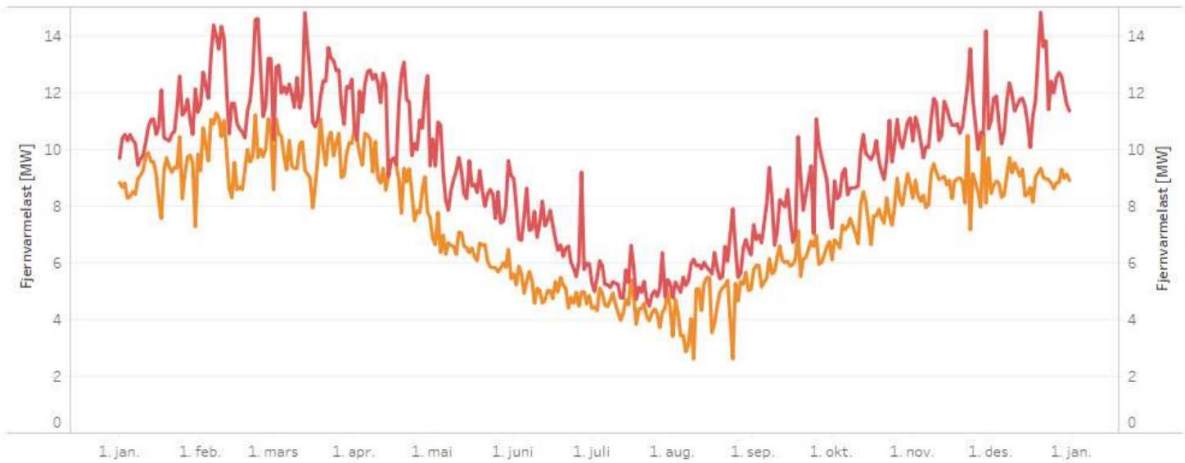


Figure 23: Min and Max daily load in Longyearbyen in 2017, district heating [19]

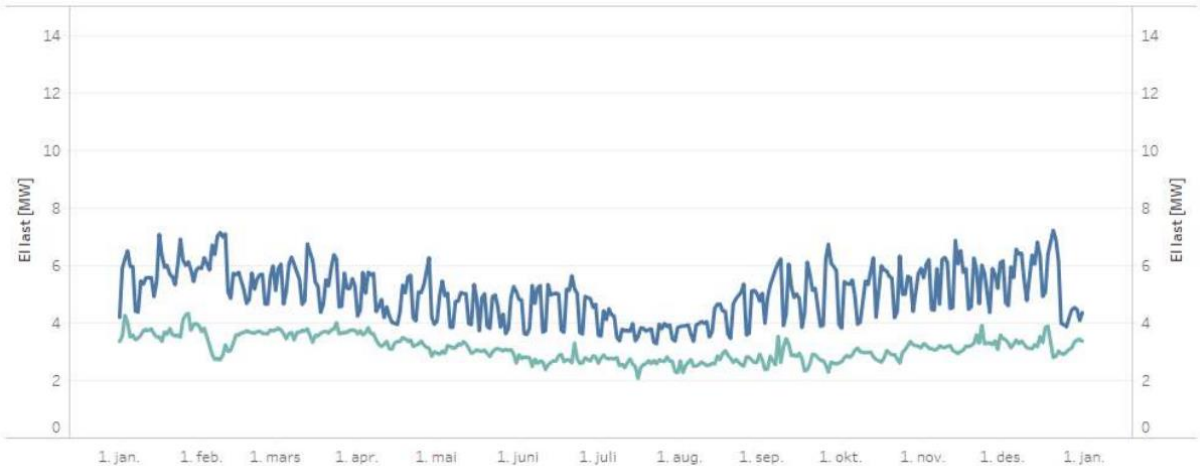


Figure 24: Min and Max daily load in Longyearbyen in 2017, electricity [19]

The many peaks in the electricity production graph are attributed to the operations at Mine 7, which supplies the coal to the power plant [22 p. 17]. They operate from 07:00 to 11:00, five days every week and is a large consumer of electricity. The reduced activity at the mine in July is illustrated in smaller peak loads in figure 24.

Based on the heat and electricity load data provided, a monthly approximation of electricity and heat production was made. Energy production and consumption is assumed to be the same. The approximation was done by multiplying the number of hours in every month, with

the average load for both electricity and heat production. The total energy production found with this method deviated only 3 % from the 110 000 MWh found by Multiconsult and can be considered a very good approximation. Scaling the whole production down by 3 % in the model let the total energy consumption match the provided data. The resulting energy production figure, expressed as watt hours, was then plotted, and can be seen in figure 25.

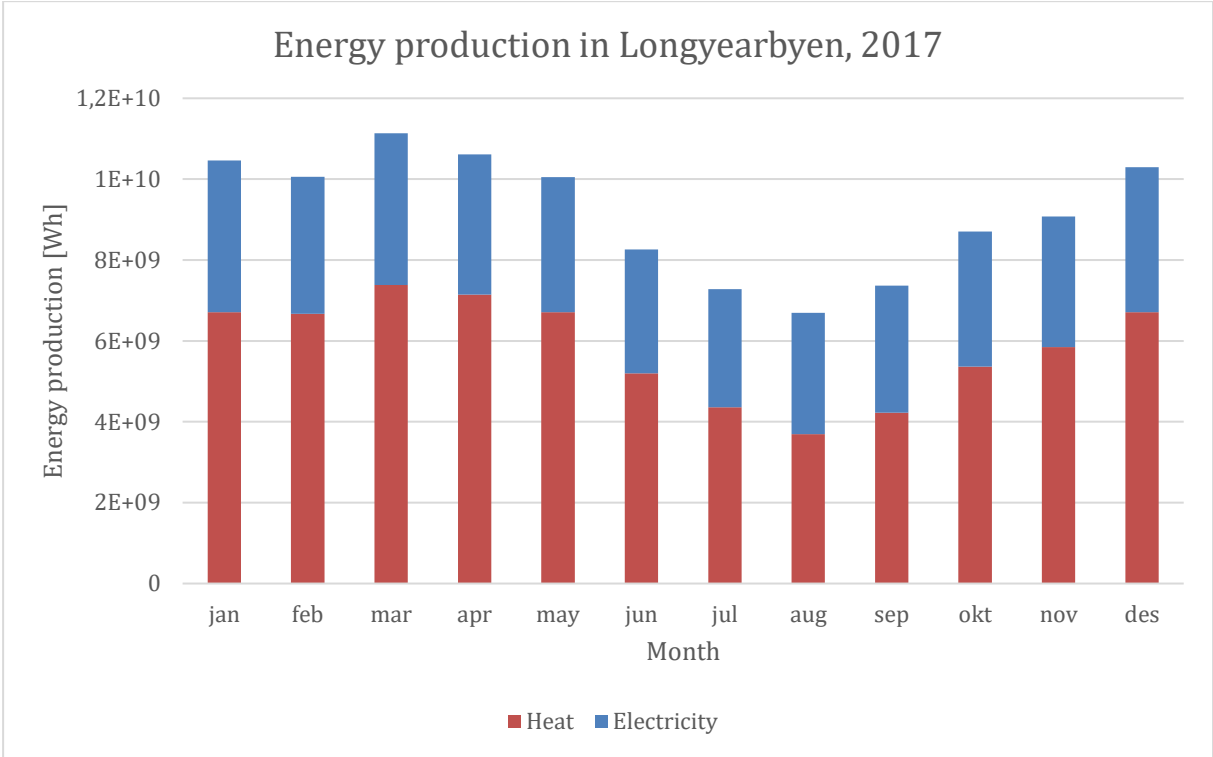


Figure 25: Monthly energy production in 2017, Longyearbyen

Having found the energy production profile of Longyearbyen, it was overlaid with the average monthly capacity factor from the Solar PV at Svalbard Airport in 2019 and 2020. A very harmonic correlation between energy demand and potential PV production can be observed from April through August in figure 26. From October through February, however, energy demand is high while production potential is zero.

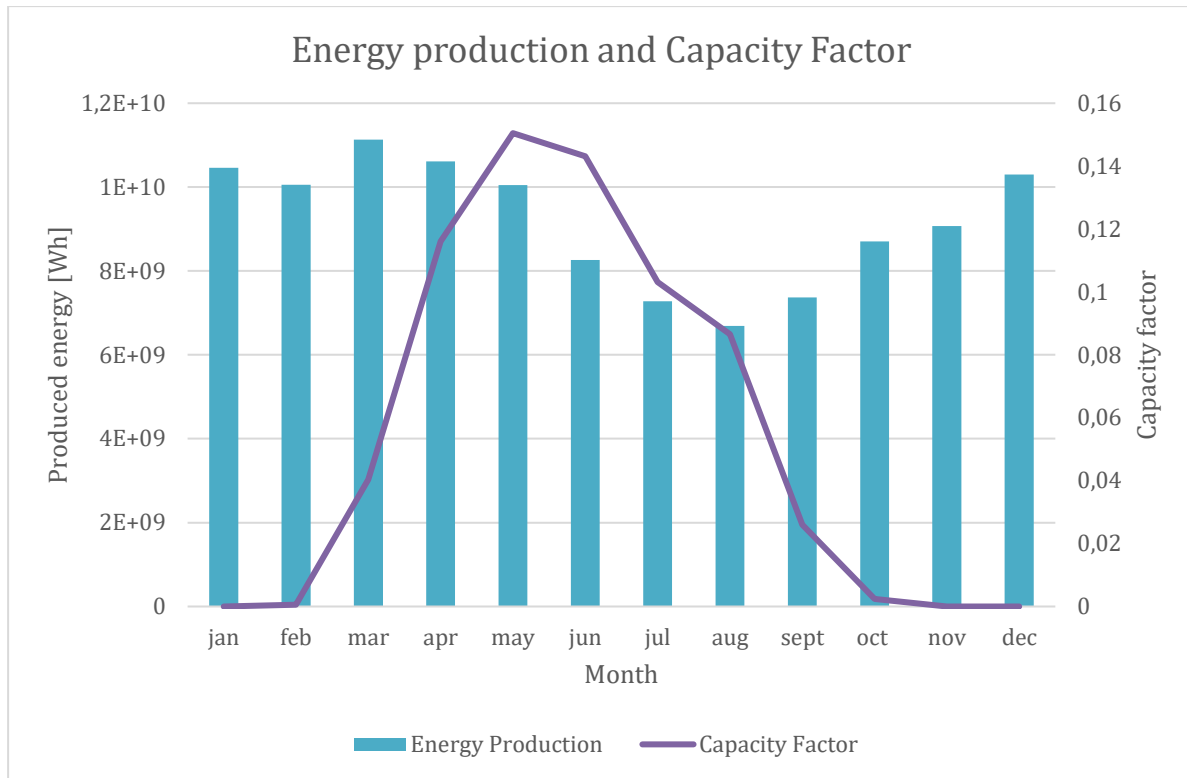


Figure 26: Monthly energy production in 2017 and average capacity factor in 2019-20, Longyearbyen

4.3.2 Full Solar Dependency

An arctic settlement with full dependency on solar energy will require a large-scale energy storage, as well as a huge solar PV production plant. Referencing figure 26, it is apparent that all energy consumed from November to February must be from storage capacity, which must be charged during the summer months. While seemingly unpractical, a simulation was run to approximate just how large of a system is required to realize it.

Having documented the energy demand of the settlement, and the capacity factor of a solar PV installation, a simulation can be run on a complete system. First, a system with 100% energy storage round-trip efficiency was simulated. The required installed capacity of a solar facility can be calculated using the energy demand and capacity factor:

$$W_p = \frac{110 \text{ GWh}}{(24 \text{ h/day} \cdot 365 \text{ day/y}) \cdot 0.0560} = 224.2 \text{ MW}_p$$

Energy production was calculated by multiplying the monthly capacity factor with number of days in the month, and the kW_p of the solar facility found above. The monthly change in stored energy is calculated by subtracting the monthly consumption from the production. In months of over-production, energy gets stored, and vice versa. Two years of simulation was plotted in figure 27, with an initial 15 GWh stored in the storage system.

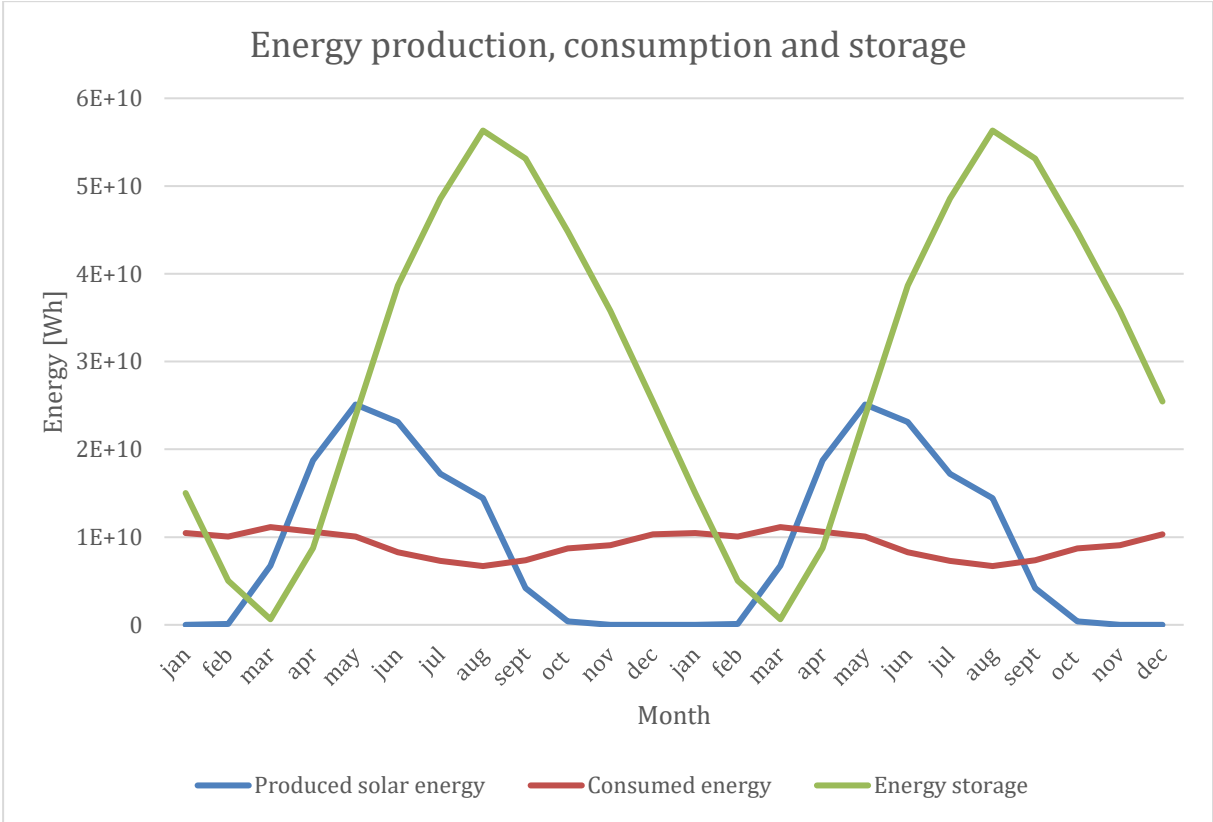


Figure 27: Two-year simulation of a fully reliant solar PV Longyearbyen. Round-trip efficiency in storage 100%

The simulation shows that a storage system with a capacity of 55.7 GWh is required to provide year-round energy, calculated by subtracting the minimum storage from the maximum. It has to be partnered with a 224 MW_p solar PV installation. This of course assumes a 100% round-trip efficiency, which is impossible. Introducing a more realistic round-trip efficiency of 60% to the storage system, which is a reasonable efficiency for modern CAES systems [43 p. 12-13], the situation changes.

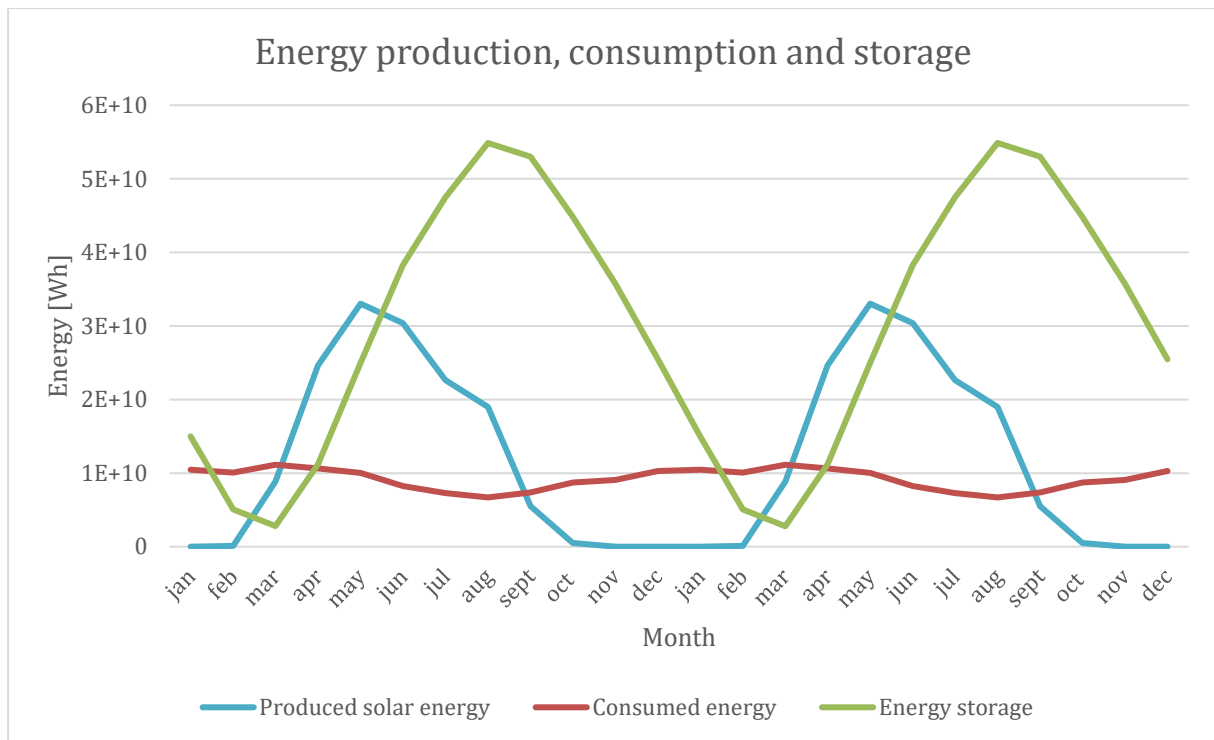


Figure 28: Two-year simulation of a fully reliant solar PV Longyearbyen. Round-trip efficiency in storage 60%

To simulate a storage system with a round-trip efficiency of 60%, the produced energy was first spent to meet the consumption. Any excess production went to storage with 60% efficiency. If consumption was higher than production, the remaining energy was taken from the storage system. Required capacity of the solar PV facility was tuned in the simulation until the system budget was zero. It shows that the required solar PV capacity had to increase to 295 MW_p, from the 224 MW_p in the system with 100% round-trip efficiency in the storage system. Figure 28 shows two years of simulating the system, starting at 15 GWh of energy stored. The required storage capacity is, surprisingly, slightly reduced to 52.1 GWh, compared to the last simulation. This is equal to 47.4 % of the total annual energy demand.

295 MW_p of solar PV will produce 144.7 GWh of solar energy annually, considering a capacity factor of 5.6 %. This means that a total of 34.7 GWh, or 24.0 % of the total produced energy is lost in energy storage processes.

4.3.3 Peak Load Energy Production and Storage

Having looked at the example with full solar PV dependency, smaller applications of solar energy had to be explored. Longyearbyen has, in later years, seen capacity at the coal power plant explode [20]. The energy demand cannot be met by the coal power plant alone, and therefore emergency back-up must be used to meet the demand. The emergency back-up consists of three 1.8 MW diesel generators, each delivering around 1.5 MW in stable output [22 p. 22-24].

2020 had an average of 6 hours of production every day of the winter from the backup generators near the city center [20]. Winter is assumed to be November through March. Assuming that, on average, 2 of the 3 generators were producing during these hours, this means that for 6 hours every day of the winter season, the generators ran at 3000 kW. The total amount of energy produced will then be:

$$E_{emergency} = 3000 \text{ kW} * 6 \text{ h/d} * 150 \text{ d} = 2.7 \text{ GWh}$$

Meaning that 2.7 GWh of energy is produced annually by the emergency generators of Longyearbyen.

The provided number is only the average. In reality the generators run only at times with high energy demand. This is mainly on the coldest days when heat and electricity demand is higher than on warm days. The simulation assumes a simplified average of 6 hours per day.

Efficiency of the storage system is assumed to be 60%, and the produced energy is consumed before stored energy. Two years of simulation is plotted in figure 29.

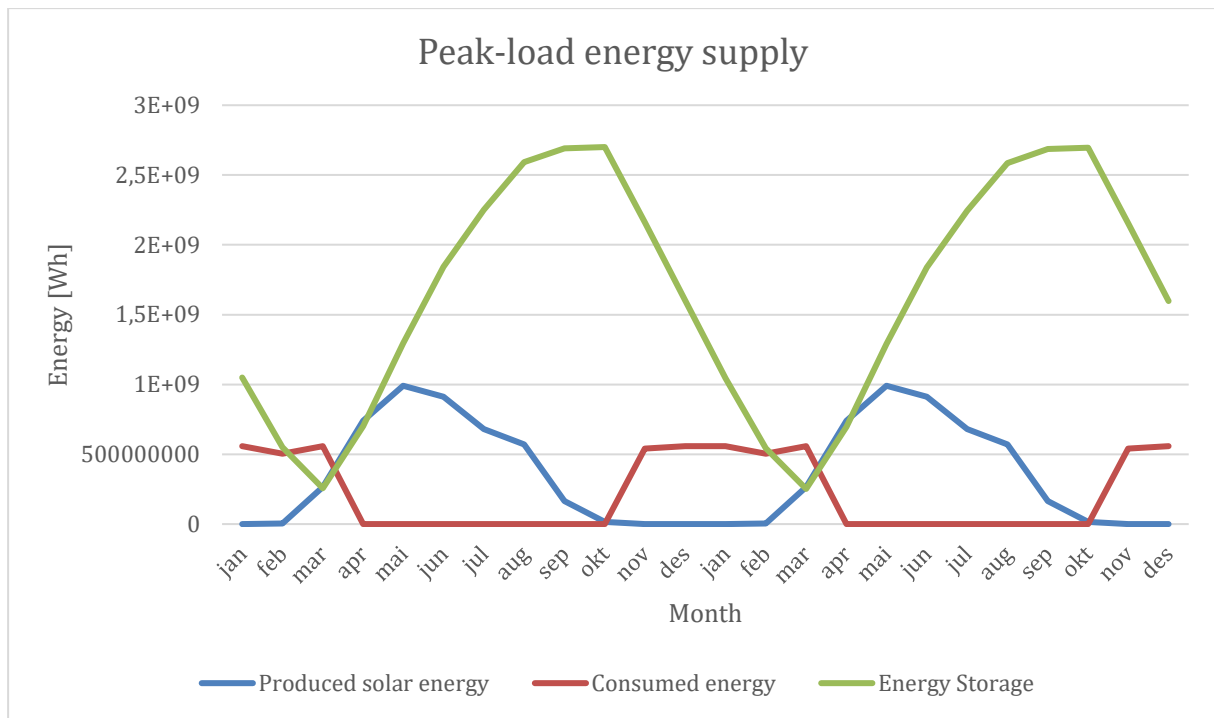


Figure 29: Peak-Load energy supplied from solar PV. Efficiency of storage 60%

The required capacity of the solar PV facility, assuming the same average monthly capacity factor as before, is 8.85 MW. In addition, the required energy storage capacity is 2.44 GWh. The simulation shows that peak energy demands happen at times where the solar resource is unavailable, and therefore it appears unattractive. With a solar PV installation of 8.85 MW_p, and a capacity factor of 5.6%, a total of 4.34 GWh is produced annually. 1.64 GWh, or 37.8 % is lost in storage processes. This is only slightly less than the 40% that would have been lost if all produced energy went through the storage system. February and March are the only months where some of the produced energy goes directly to the cause.

4.3.4 Summer-Only Solar Dependency

The complementary relationship between solar capacity factor and energy demand in the months from April through August, as demonstrated in figure 26, makes summer-only solar energy an attractive alternative. The idea behind this simulation, is to rely solely on solar PV energy in the summer and use the existing energy supply to supply energy in the winter. This reduces the dependence on fossil fuel in the summer. Life expectancy of installed energy will

increase, and maintenance on the systems can be performed during downtime. The need to run the existing system at suboptimal loads and reduced efficiency is also decreased.

To be able to supply a solar dependent system which runs only in the summer months, certain storage will be required to combat the intermittency. There is the obvious night/day intermittency, or rather the sun being in front or behind the panels in the arctic summer, as well as longer periods of bad weather conditions for solar production. The average daily capacity factor for the months in between April and August in 2020 was found to be 11.97%, with peaks of over 25% on the best days, and the worst days at around 1%. Figure 30 illustrates the variation in capacity factor in 2020, where longer periods of low capacity factor can be observed.

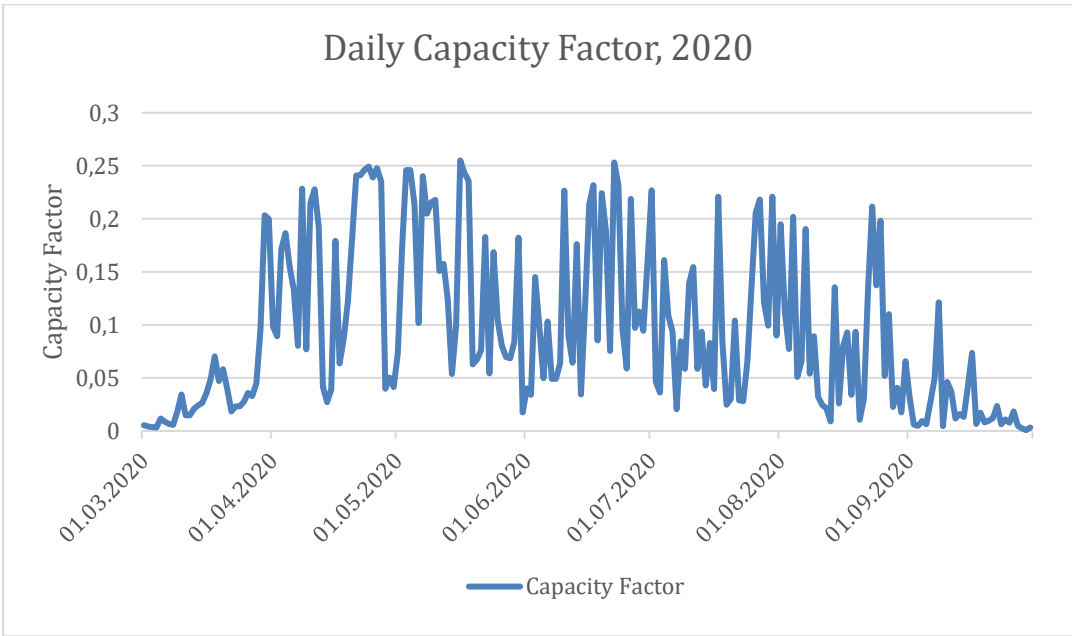


Figure 30: Daily capacity factor from March 1st to September 30th at Svalbard Airport

To supply a stable energy supply, some energy would need to go through a storage process before consumption. There will always be efficiency losses in the storage process, and therefore it should be avoided. The simulation assumes that all electricity that is produced from solar when the production is lower than consumption, is consumed at 100% efficiency. On days with a surplus production, the energy first meets the consumption. Then, the surplus energy is sent to storage, with efficiency losses in compliance with the chosen storage technology.

With the daily consumption figure in mind, a model was made where all production which exceeded daily consumption would undergo an efficiency loss of 60%. This is to simulate a realistic scenario with CAES technology. The installed solar PV capacity was then tweaked until the total energy production matched the consumption of the period. Simulation revealed that this would require a total PV capacity of 86.3 MW_p. This is equivalent to 263 914 Sunpower E20-327 panels. The simulation, seen in figure 31, also revealed that the required storage capacity is 2.76 GWh – Peak stored energy minus the minimum level. To avoid draining the storage system by the end of April, approximately 1.5 GWh must be stored by the start of solar-only dependency.

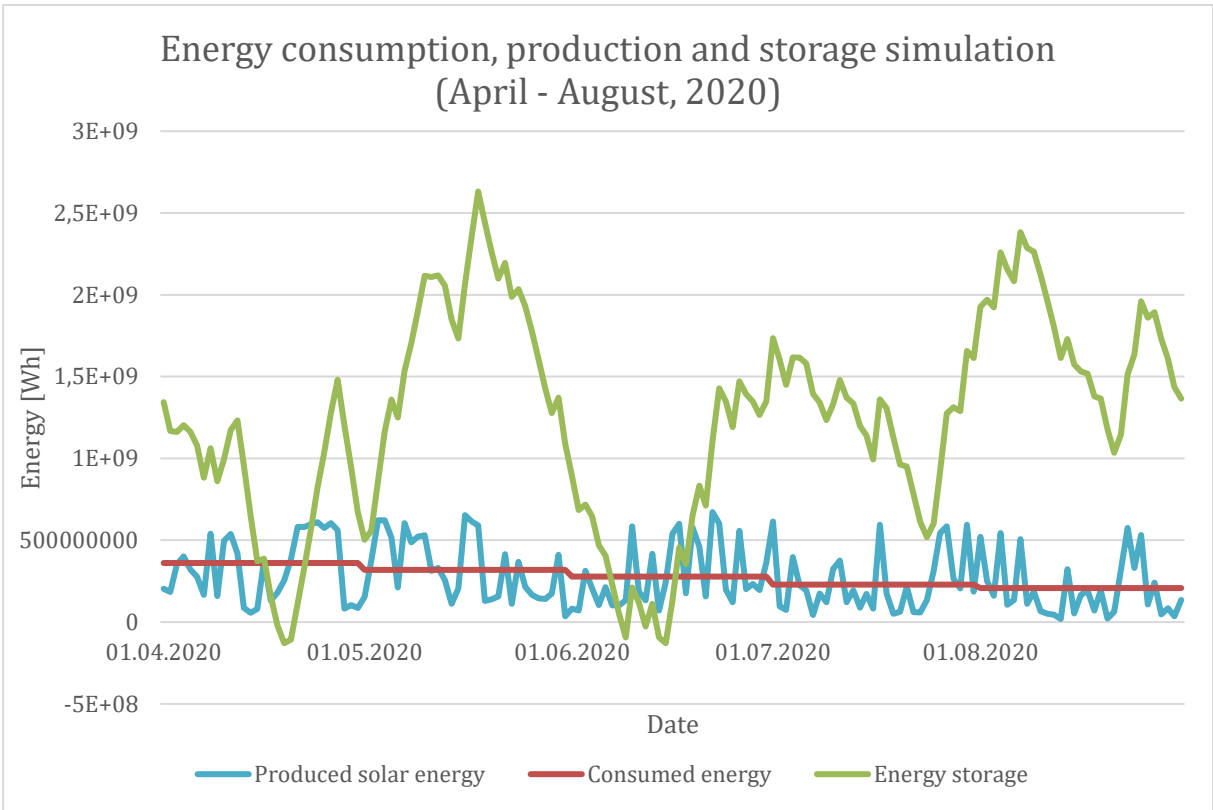


Figure 31: Simulation of a fully solar reliant Longyearbyen in 2020. Efficiency of storage 60%

A weakness in this simulation is that the energy demand is assumed to be uniform throughout the month. Realistically, the tendency is that on days where the solar resource is abundant, energy demand decreases. This means that days of low solar production also might have a higher energy demand. It is therefore fair to assume that the capacity of solar PV and storage must be higher than the simulation suggests, because the intermittency is amplified by the

inverse correlation. In addition, it does not account for the variation in energy production and demand throughout the day. The tendency is that during daytime, the energy demand is larger than in the night.

Total energy loss is calculated similarly to earlier simulations. The total consumed energy from April 1st to August 31st is 42.61 GWh. A solar installation with a capacity of 86.3 MW_p would, in the same period in 2020, produce 37.94 GWh. 89.04% of the produced solar energy would be consumed, and only 10.96 % lost in energy storage processes.

An added benefit of the solar system for the summer months is that the energy storage system can be used to offload the generator at the peaks in the winter months, and possible emergency-generator running might become unnecessary. The storage capacity required for a system with 86.3 MW_p of solar installed, is 2.76 GWh. This is slightly more than the simulated storage capacity in sector 4.3.3.

4.3.5 Combining Summer Solar and Peak Storage

Considering April through August as solar-only, March and September would have had some wasted solar potential. This was added to the previous model of full solar dependency during the summer months, where 100% of the produced solar energy in March and September went to storage with 60% round-trip efficiency. The simulation shows a good potential for combining full summer solar dependency, and winter peak energy. Starting with empty storage in March, the production during March was almost enough to cover the lower production periods in the start of the year. The production in September was enough to almost fill the storage capacity, and the solar PV season ended with 2.152 GWh in energy storage (figure 32). This capacity could help cover the peak-production hours during winter season. 2.44 GWh was required to cover the entire winter season of peak-load energy storage, and avoid running emergency-generators, as shown in figure 29.

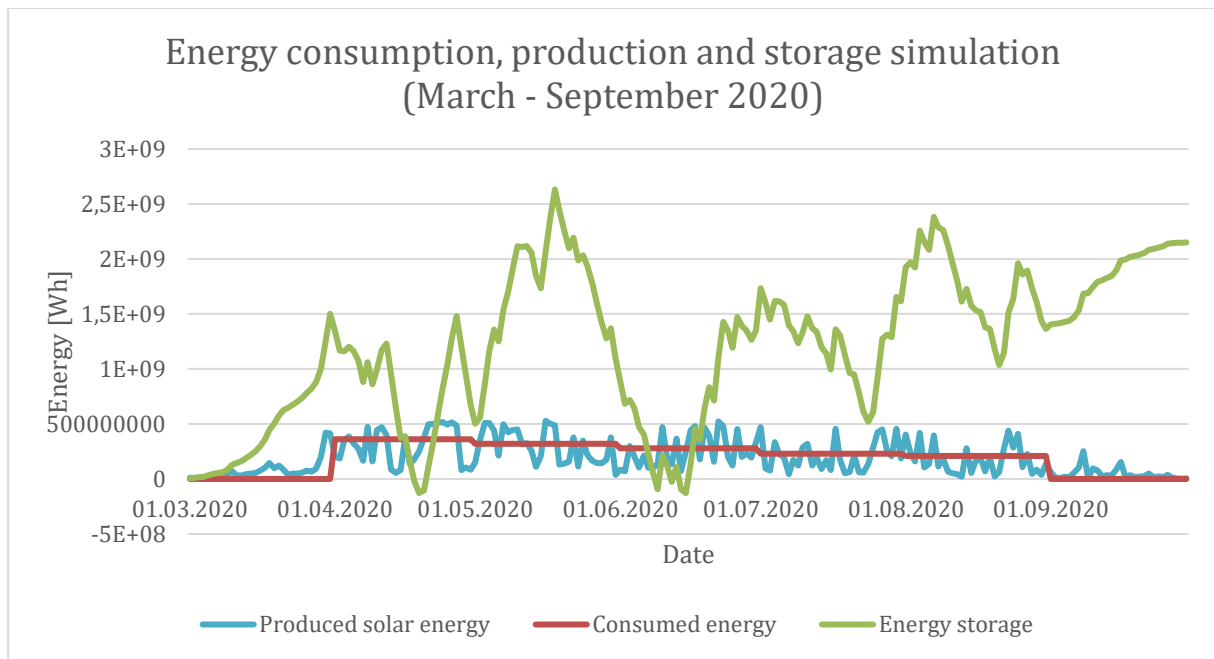


Figure 32: Simulation of a fully solar reliant Longyearbyen in 2020. Energy produced from solar in March and September are sent to storage for peak-load supply in winter. Efficiency of storage 60%

Comparing this simulation to the peak-load only variant, the solar PV capacity is almost 10 times bigger. However, the installed storage capacity is only increased by 0.288 GWh. It would allow for 153 days of full solar dependency in Longyearbyen, while also supplying energy at peak production in the winter season to avoid using emergency capacity.

With 153 days of full solar dependency, the existing energy supply would have to run for only 58% of the year. It is therefore assumed that this increases lifetime by 42%. The turbines at the coal power plant in Longyearbyen have approximately 20 years left of their predicted lifetime [19 p. 21]. This would increase to more than 28 years. In addition, maintenance could be performed over the idle period, further increasing lifetime. Realistically, as the simulated system would take a long time to implement, it is more beneficial to look at the lifetime of the new system that will be installed as the coal plant is retired.

4.4 Cost of Energy in the Arctic

The coal power plant in Longyearbyen is entirely supplied with coal from Mine 7 in Longyearbyen. Mine 7 is the last operating Norwegian coal mine [67]. The power plant has had a budget of around 112 – 128 Million NOK in 2018 to 2020, and is predicting a budget of 128 Million NOK in the coming years [68 p. 56]. In addition, Mine 7 receives significant financial support from the Norwegian government to keep the operations running. In 2020, this figure is 40 Million NOK, but this is an outlier because of maintenance work in relation to flooding in the mine [67]. However, Longyearbyen Lokalstyre expects the annual deficit to be around 35-40 Million NOK in the coming years as well [69]. In total, this yields annual expenses of ~160-170 Million NOK for operation of the coal power plant.

An annual energy production of 110 000 MWh is produced from the coal power plant in Longyearbyen [22 p. 13]. This results in a cost of approximately 1.5 NOK / kWh. The low cost of the energy is mainly caused by the high efficiency of the coal power plant when the heat is being utilized as well as it is. With only 40 000 MWh being electricity, electricity cost is 4 NOK / kWh.

For private customers in Longyearbyen, electricity prices are decided by Longyearbyen Lokalstyre. There are several fixed costs related to the electricity meters and grid rent. The running costs depend on annual consumption. Base price in 2020 is 1.98 NOK/kWh, increasing to 2.40 NOK/kWh if consumption exceeds 50 000 kWh annually [70 p. 5]. The price of district heating is 0.47 NOK / kWh [70 p. 5].

As found in section 2.2.2, 8.183 GWh of energy is consumed in Ny-Ålesund annually. Assuming a diesel price of 12 NOK/l [22 p. 16], this means that the price of diesel energy in Ny-Ålesund is:

$$\frac{1\ 000\ 000\ l \cdot 12\ NOK/l}{8\ 183\ 000\ kWh}$$

1.47 NOK/kWh, only accounting for fuel costs.

4.4.1 Cost of Energy Storage

It is established that storage is an important component in renewable energy systems. Energy storage is also possible to implement storage in fossil energy systems to maintain consistent and efficient loads. A 2017 report conducted by The International Renewable Energy Agency, IRENA, performed a cost and market analysis from now until the year 2030 [46].

The cost of storage systems suggested in this thesis were USD 53/kWh, or around 450-500 NOK/kWh for CAES systems. However, a share of 40% of this estimation is allocated to excavation of a suitable cavern [46 p. 57]. As these caverns already exist at the Svalbard settlements, in the form of abandoned coal mines, this cost can be drastically reduced. To limit leakage, airtight bags can be installed in the chambers to better contain the pressurized gases [42 p. 2]. Some excavation is to be expected, in addition to sealing off the chambers, so this cost estimation will reduce chamber excavation costs by 75%. The new estimated price is then around 350 NOK/kWh of storage.

4.4.2 Cost of Solar Photovoltaics

Solar photovoltaics has seen an aggressive price decline in the later years. Figure 33 shows the estimated December prices for solar PV in Europe, in EUR/W_p. A sharp decline by up to 18 % for Bifacial modules in 2020 is seen, and a slight decrease since October. The prices are shown before taxes, and relevant taxes for the country that will order the PV panels must be applied. VAT for electronics to Norway is 25% [71], but Svalbard is exempted from toll because of the Svalbard Treaty [72]. Euro conversion rate is assumed to be 10.63 EUR/NOK, as was the case December 1st, 2020 [73]. The calculated prices are shown in table 4.

Module class	€/Wp	Trend since October 2020	Trend since January 2020	Description
Crystalline modules				
Bifacial	0.32	+ 3.2 %	- 17.9 %	Solar modules with bifacial cells, transparent back sheets or double glas modules, framed or unframed.
High Efficiency	0.31	+ 3.3 %	- 3.1 %	Crystalline modules 330 Wp and above with PERC, HJT, n-type or back-contact cells, or combinations thereof
All Black	0.31	+ 3.3 %	- 6.1 %	Module types with black back sheets, black frames and a rated power between 290 Wp and 390 Wp
Mainstream	0.22	+ 4.8 %	- 12.0 %	Standard modules, typically with 60 multicrystalline cells, aluminum frame, white backsheets and 275 Wp to 325 Wp
Low Cost	0.15	0.0 %	- 11.8 %	Factory seconds, insolvency goods, used or low-output modules (crystalline), products with limited or no warranty

Source: www.pvxchange.com

NOTES ON READING THE PRICE INDEX

1. Only tax-free prices for photovoltaic modules are shown.
2. The prices stated reflect the average prices quoted on the European spot market (customs cleared).

Figure 33: Solar PV prices in December 2020. Tax-free prices, and modules only [62]

Table 4: Cost of solar PV per W_p , converted to NOK and accounting for taxes

	Base price, and Svalbard	Mainland Norway
Bifacial	3.40	4.25
High efficiency	3.30	4.13
Mainstream	2.34	2.925
Low cost	1.59	1.99

The costs are panels only, and PVexchange estimates that finished solar PV installations in Germany will be 4-6 times the cost [62]. For this thesis, 6 times the cost of panels for finished installations is assumed.

4.5 Economic Impact

4.5.1 Svalbard Airport

Assuming an average linear decrease in efficiency from 100% to 85% after the minimum lifetime of 25 years, gathered from figure 15, and an annual inflation rate of around 2.25% [74], it can be calculated approximately how much money the airport in Longyearbyen will save over the lifetime of the installed solar power plant. The capacity factor has been around 5.65% the first two years of full production. Longyearbyen Airport is a large energy consumer at 1540 MWh in 2017 [22 p. 17] and pays the full 2.40 NOK/kWh [70 p. 5].

If the inflation is in line with forecasts, the electricity price will increase from 2.4 NOK/kWh to almost 4.1 NOK/kWh after 25 years. The capacity factor will decrease from 5.65% to 4.80% due to degradation. During the first year of the installation, 163 805 NOK was shaved of the electricity expenses. This figure will be 237 502 NOK in the 25th year. In total, the savings are estimated to be around 4 972 269.

Svalbard Airport has 39 750 W_p of “mainstream” solar PV capacity, and 98 100 W_p of “high efficiency” solar PV capacity. In December 2020 prices, this would equal an initial cost of 416 745 NOK. The investment was made several years ago, though. Assuming the July 2017 price [75], as an average price of the three expansions, the same cost would have been approximately 700 000. In addition, 11 inverters from 10 to 20 kW, wires, and frames would have to be installed. Lastly, the labor to install and the system must be accounted for. Assuming a 6-fold increase in price for the full installation [62], the installation in 2017 would have cost 4.2 million NOK. Lifetime saving from the installation on Svalbard Airport is, in that case, estimated to be around 800 000 NOK. This is equal to a return on investment (ROI) of 18.4 % after 25 years.

4.5.2 Private Installations

With the numbers from the airport in mind, similar estimations can be made to assess the potential for private installations. Smaller customers pay 1.98 NOK/kWh of electricity [70 p. 5]. A simulation like the one made for the airport installation was made, using the capacity factor from southwest-facing wall-mounted panels, for both monocrystalline and

polycrystalline. The capacity factor is gathered from table 3. 6.03 % for monocrystalline, and 5.65 % for polycrystalline. Assuming degradation rates in line with figure 15, capacity factor drops to 5.29 % and 4.69 % respectively after 25 years. Electricity price increases to 3.38 NOK/kWh.

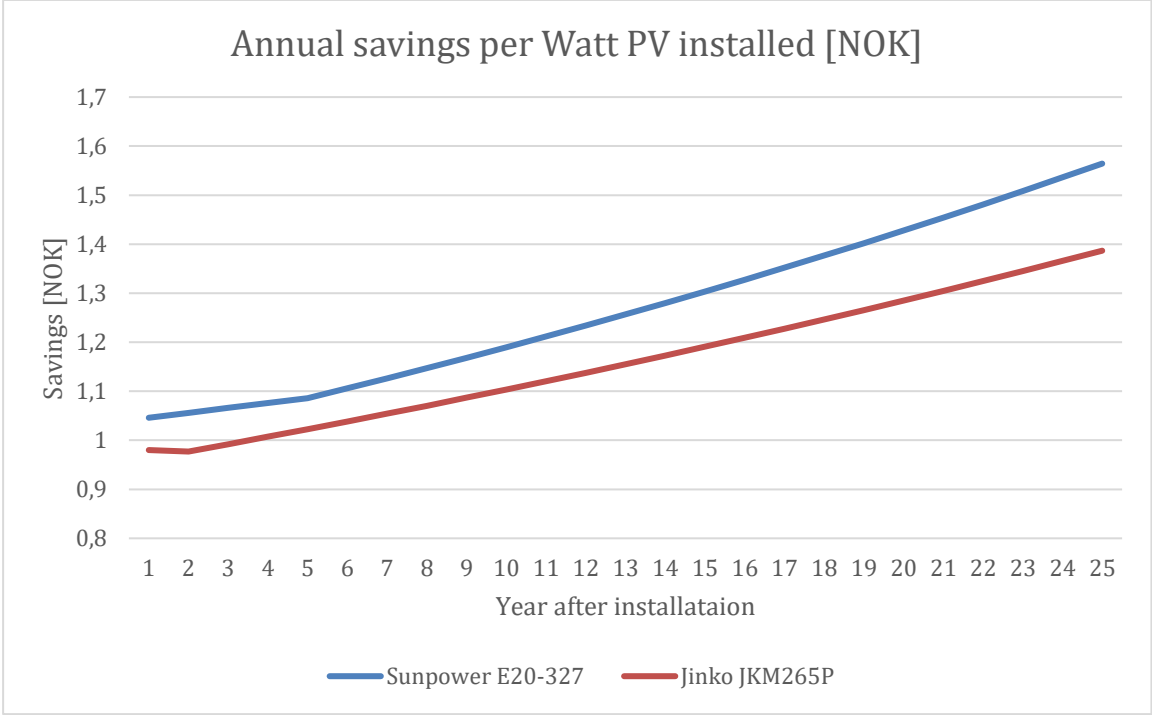


Figure 34: Annual savings in NOK per W_p installed in Longyearbyen for private installations

Figure 34 shows the annual savings in NOK per installed watt of solar PV for the monocrystalline Sunpower E20-327, and the polycrystalline Jinko JKM265P. Accumulated, this adds up to total savings of 31.8 NOK per W for monocrystalline, and 29.1 NOK for the polycrystalline panels. For the 327 W Sunpower E20-327 this will equal 10 399 NOK in savings per panel, while the 265 W Jinko JKM265P will have a lifetime saving of 7712 NOK. Assuming a December 2020 solar PV price, and the price increasing by 600% for the full installation [62], Sunpower E20-327 panels will save NOK 3924 per panel Jinko JKM365P will save around 3991 per panel.

4.5.3 Full Solar Dependency

Full solar dependency required a total energy storage of 52.1 GWh, and a solar PV installation of 295 MW_p. At 350 NOK/kWh for CAES systems, and 14.04 NOK/W_p for mainstream solar PV, the cost of fully supplying Longyearbyen with year-round Solar PV is:

$$\begin{aligned} & 52.1 \text{ GWh} \cdot 350 \text{ NOK/kWh} + 295 \text{ MW}_p \cdot 14.04 \text{ NOK/W}_p \\ & = 2.24 \cdot 10^{10} \text{ NOK} \end{aligned}$$

Yielding a total price of 22.4 Billion NOK. The installation would remove the need for any other energy sources on the island, bar some emergency energy. The system would completely end the need for fossil fuel, and the coal power plant could be shut down. Assuming annual expenses of 165 MNOK from the coal power plant, and an inflation rate of 2.25 % [74], total savings over 25 years would be 5.47 Billion NOK. The net result is a loss of 16.94 Billion NOK, a negative ROI of 410 %. A very unattractive option, in other words.

4.5.4 Summer-Only Solar Dependency

For a summer-only solar dependent Longyearbyen, the simulated storage capacity is 2.152 GWh, and the solar PV system 85.3 MW_p. Assuming the same prices as before:

$$\begin{aligned} & 2.152 \text{ GWh} \cdot 350 \text{ NOK/kWh} + 85.3 \text{ MW}_p \cdot 14.04 \text{ NOK/W}_p \\ & = 1.951 \cdot 10^9 \text{ NOK} \end{aligned}$$

Yielding a total cost of 1.951 Billion NOK. There would still be a need for an energy system with the same capacity as today's power plant, but it would be running for only 58% of the year. Emergency generators would still need to be installed, but not used to the extent of today. 42.61 GWh of the annual 110 GWh produced in Longyearbyen would have been produced by the solar PV facility. A quick estimation, assuming that the expenses and production at the coal power plant in Longyearbyen are directly related, finds the annual savings to be 63 915 000 NOK, considering current annual expenses of 165 000 000 NOK. This results in savings of 2.114 Billion NOK after the 25-year lifetime of the solar power plant. Net result is savings of 163 Million NOK, or an ROI of 7.71 % after 25 years.

4.6 Climate Impact

In addition to being an economically competitive energy source globally, solar PV has beneficial properties to combat the ongoing global climate changes. After production and installation, the CO₂ footprint of solar PV is practically zero. The 2014 IPCC report estimated the carbon footprint of several energy sources, as grams of CO₂ equivalents per kWh [76 p. 1335]. The median values from relevant technologies are listed in table 5.

Table 5: Carbon footprint from different energy sources [76 p. 1335]

Technology	Carbon Footprint [gCO ₂ eq. / kWh]
Coal	820
Solar PV – Rooftop	41
Solar PV – Utility Scale	48
Wind onshore	11

To properly calculate the carbon footprint of energy sources in the Arctic, the increased efficiency from heat utilization must also be factored in. The IPCC report assumes a median efficiency of 39 % for coal power plants [76 p. 1333]. The efficiency of the coal power plant in Longyearbyen is complex because there are two turbines, one which is producing electricity and heat at efficiencies of 19 % and 63 % respectively, while the second turbine only produces electricity at 27 % efficiency [19 p. 21].

To estimate efficiency, the coal consumption at the power plant was compared to the energy production. Multiconsult states an energy density of 700 kcal/ton on the coal consumed in Svalbard [19 p. 21]. It is assumed that this is a prefix error, and that the correct figure is 7 Gcal/ton, which is in line with figures found online [77]. Considering that 1 kcal equals 4184 J, or 1.162 Wh, this equals:

$$7 \text{ Gcal/ton} * 4184 \text{ J/kcal} * \frac{1}{3600} \text{ Wh/J}$$

= 8.134 MWh/ton. Annual coal consumption is between 25 to 29 000 tons. Assuming an average of 27 000 tons in 2017, this means that annually, 219 618 MWh of coal is consumed to produce 110 000 MWh of energy. The total efficiency of the coal power plant in Longyearbyen is therefore estimated to be 50.1 %.

In Ny-Ålesund, the diesel generators are producing electricity at an efficiency of 41.7 %. If waste heat utilization is included, the total efficiency is 76 % [22 p. 6]. Diesel has a specific density of 0.85 kg/l [23], an energy density of 12 667 Wh/kg [24] and a CO₂ production of 3.153 kg CO₂/kg [78] when combusted. This means that at 100% efficiency, 249 g CO₂ eq. / kWh is released by diesel power. Under normal conditions, this figure is divided by 0.417, and in Ny-Ålesund by 0.76, yielding 597 and 328 gCO₂ eq. / kWh respectively. For coal, the carbon footprint for improved efficiency was calculated as following:

$$\begin{aligned}
 CO_2 \text{ eq.}_{arctic} &= CO_2 \text{ eq.}_{global} \cdot \frac{\eta_{global}}{\eta_{arctic}} \\
 &= 820 \text{ gCO}_2 \text{ eq./ kWh} \cdot \frac{0.39}{0.501} \\
 &= 639 \text{ gCO}_2 \text{ eq./ kWh}
 \end{aligned}$$

Taking these improved efficiencies into consideration, the carbon footprint of the two energy sources is reduced. Efficiency of coal is increased by 28.46 % from 0.39 to 0.501, while the efficiency of diesel is increased by 82.25 % from 0.417 to 0.76. The updated carbon footprints in table 6 reflects this efficiency increase.

Solar must also be corrected for arctic conditions. IPCC assumes an average FLH of 1750 for solar PV [76 p. 1333]. FLH is short for Full Load Hour. With every year having 8760 hours, an FLH of 1750 is equal to a capacity factor of 20%. It is established that solar in the Arctic has a capacity factor of around 5.6%, translating to an FLH of 491. CO₂ equivalents were calculated similarly to the coal value, by multiplying by the efficiency relation 0.20/0.056, the ratio between IPCC's capacity factor and the capacity factor in the Arctic. Results are added to table 6.

Table 6: Carbon footprint from different energy sources in arctic conditions

Technology	Carbon Footprint [gCO ₂ eq. / kWh]	Carbon Footprint [gCO ₂ eq. / kWh], arctic conditions
Coal	820	639
Diesel	597	328
Solar PV – Rooftop	41	146
Solar PV – Utility Scale	48	171

The results in table 6 are both surprising and interesting. On a global average, replacing coal and diesel energy with utility scale solar PV reduces emissions by 1700 % and 1240 % respectively. Under arctic conditions, this is reduced to 374 % and 192 %. The climate impact from solar PV is reduced immensely under arctic conditions.

4.6.1 Svalbard Airport

The Svalbard Airport solar PV facility can expect to produce around 1 578 332.726 kWh during its lifetime if accounting for degradation. The solar PV, with a carbon footprint of 146 g CO₂ eq. / kWh will directly replace coal electricity, with a carbon footprint of 820 g CO₂ eq. / kWh. Total CO₂ equivalents saved during the lifetime is therefore:

$$(820 \text{ gCO}_2/\text{kWh} - 146 \text{ gCO}_2/\text{kWh}) \cdot 1578332.726 \text{ kWh}$$

$$= 1064 \text{ tons CO}_2 \text{ eq.}$$

Meaning that a total of 1064 metric tons of CO₂ equivalents will not be emitted, thanks to the solar PV facility at Svalbard Airport alone.

4.6.2 Private installations

The figure for private installations is similar to the airport figure. In addition, the figure for replacing diesel generated energy will be included. As many arctic settlements, like Ny-Ålesund and Sveagruva, are diesel-powered, it is highly relevant.

Assuming degradation and capacity factor in line with the installed solar PV at Svalbard Airport, monocrystalline solar cells will produce 12.2 kWh per installed watt in its lifetime. The figure for polycrystalline is 11.19 kWh / W. Applying the same calculations as for the airport yields the results presented in table 7.

Table 7: Climate impact of installing solar PV in the Arctic to replace electricity

	Replacing coal	Replacing diesel
Monocrystalline	8.22 kg CO ₂ eq. / W _p	5.50 kg CO ₂ eq. / W _p
Polycrystalline	7.54 kg CO ₂ eq. / W _p	5.05 kg CO ₂ eq. / W _p

4.6.3 Full Solar Dependency

Assuming full solar dependency in Longyearbyen, all coal would be replaced by utility-scale solar power. The calculation is simple:

$$\begin{aligned}
 & (639 \text{ gCO}_2/\text{kWh} - 171 \text{ gCO}_2 \text{ eq.}/\text{kWh}) * 110\,000 \text{ MWh} \\
 & = 51480 \text{ tons CO}_2 \text{ eq.}
 \end{aligned}$$

Meaning that fully supplying the Longyearbyen settlement with solar power will save 51480 tons of CO₂ equivalents annually.

4.6.4 Summer-Only Solar Dependency

A summer only solar dependent society in Longyearbyen would save 153 days of energy production from coal, equaling 42.61 GWh annually. Calculation is similar to the above calculation:

$$(639 \text{ gCO}_2 \text{ eq./kWh} - 171 \text{ gCO}_2 \text{ eq./kWh}) * 42610 \text{ MWh}$$

$$= 19941 \text{ tons CO}_2 \text{ eq.}$$

Meaning that the facility would save 19941 tons of CO₂ equivalents annually. Considering the benefit of installing storage capacity to replace spike-load energy production by diesel in the winter, the following can be added:

$$2.7 \text{ GW}_h \cdot (328 - 171) \text{ gCO}_2 \text{ eq./kWh}$$

$$= 424 \text{ tons CO}_2 \text{ eq.}$$

Giving a total CO₂ reduction of 20365 tons for the suggested system.

4.7 Discussion

The research conducted in the thesis has revealed that there is a potential for solar PV production in arctic conditions. Small, private, installations are proven to be financially viable, with the potential increasing as PV prices continue to decline. The challenge with solar PV in small power grids, is that the intermittent nature of solar energy is interfering with the energy demand of the existing power supply. This damages the existing supply. Energy storage systems are an integral part of energy systems with renewable energy, and the importance is even higher in the Arctic.

Compressed Air Energy Storage is suggested as a potential storage system in the thesis. The infrastructure to install it already exist in the form of abandoned coal mines. Existing systems, for example in Germany, are proven to have relatively high round-trip efficiencies. For daily cycles, and maybe up to weekly, CAES has proven potential. However, the optimal discharge time for CAES is between hours up to days [43 p. 2]. The long-term potential of the storage system, for example for peak-energy storage, is therefore questionable. When Longyearbyen Lokalstyre surveys the potential for energy storage to stabilize energy load, CAES is an option that deserves serious consideration.

From a climatic point of view, solar PV in the Arctic replaces coal and diesel energy, which are huge contributors to the increasing CO₂ concentration in the atmosphere. The system

suggestions in the thesis, as well as the already existing PV system at Svalbard Airport, are proven to save tons of CO₂ equivalents. Climate change, being a global challenge, requires global solutions. Compared to the global average, the efficiency of fossil energy is high in the Arctic because of the heat utilization. Meanwhile, solar PV performs worse in the arctic than the global average. Table 6 illustrates this in a good way. The carbon footprint is only reduced by 73.3 % for coal and 47.9 % for diesel in the Arctic. The global mean is 94.2 % for coal and 92.0 % for diesel. It is therefore not in the best global interest to replace fossil energy in the Arctic with solar PV. That should rather be done in areas with low fossil efficiency and high solar PV potential.

Studies have shown that wind and solar energy have complimentary benefits in the Arctic [79 p. 5]. An option to reduce both the solar capacity and required energy storage capacity, is to include some wind energy in the simulations conducted in the thesis. Wind energy in the Arctic brings a whole new set of challenges and opportunities. This is outside the scope of this thesis but could prove to be a great contributor to a shift towards green energy in the Arctic.

The thesis is focused on the global effects on climate of renewable energy in the Arctic. Local environmental issues are not touched upon. The arctic nature is fragile, and intervention has long-lasting and unpredictable effects. Solar and wind installations are serious intrusions in the arctic landscape, and this must be taken into consideration if larger installations are to be built.

5 Conclusion

Data from the solar PV installation at Svalbard Lufthavn show that the average capacity factor at the facility is 5.6 % after its first two full years of production. While the production in the winter is zero, monthly capacity factors are observed to be as high as 16 % in the summer. On peak days, capacity factors of more than 30 % are observed. Predictions show that the installation will save around 800 000 NOK during its 25-year lifetime, while also reducing CO₂ emissions by 1064 tons. Several rooms for improvement are found and should be considered if bigger installations are to be built. Most notable is the tilt and orientation of panels, as well as technologies such as bifacial panels and solar tracking systems.

Simulations show that full solar reliance in the summer-season is feasible. It requires an installation of 86.3 MW_p solar PV, and 2.76 GWh of storage with 60 % round-trip efficiency. Estimations show a potential return on investment of 7.71 % after 25 years, saving 163 Million NOK. The emission reduction from the system would be 20 365 tons CO₂ equivalents.

The fragile power grids of arctic settlements have few links in the system that can equalize load fluctuations. Introduction of intermittent solar PV on even a private scale is therefore advised against until energy storage capacity is developed. Compressed air energy storage is suggested as an option for settlements on Svalbard because the required infrastructure already exists.

Because of the high heat demand in arctic settlements, efficiency of the fossil generators is higher than the global average. Longyearbyen sees efficiencies of 50.1 % in the coal power plant, and Ny-Ålesund up to 76 % for its diesel generator. Paired with low solar utilization, the climate impact of installing PV in the Arctic is lower than in areas with low fossil efficiency and high solar efficiency. Treating the climate change as the global challenge it is, it would be more beneficial to install solar PV potent areas, if climate benefit is the target.

6 Sources

- [1] Intergovernmental Panel on Climate Change, “*Headline Statements*”. Retrieved from: <https://www.ipcc.ch/sr15/resources/headline-statements/>. Date visited: 12.12.2020.
- [2] National Aeronautics and Space Administration, “*Global Temperature*”. Retrieved from: <https://climate.nasa.gov/vital-signs/global-temperature/>. Date visited: 12.12.2020.
- [3] United Nations Framework Convention on Climate Change, “*The Paris Agreement*”. Retrieved from: <https://unfccc.int/process-and-meetings/the-paris-agreement/the-paris-agreement>. Date visited: 12.12.2020.
- [4] A. Tjernshaugen, “Klima i Arktis”, *Store Norske Leksikon*, 09.12.2020. Retrieved from: https://snl.no/Klima_i_Arktis. Date visited: 10.12.2020.2020.
- [5] V. Hisdal, S. Barr, “Arktis”, *Store Norske Leksikon*, 01.12.2019. Retrieved from: <https://snl.no/Arktis>. Date visited: 15.09.2020.
- [6] A. Tjernshaugen, “Polarsirkel”, *Store Norske Leksikon*, 15.06.2020. Retrieved from: <https://snl.no/polarsirkel>. Date visited: 15.09.2020.
- [7] Time and Date, “*Annual weather averages in Leknes*”. Retrieved from: <https://www.timeanddate.com/weather/norway/leknes/climate>. Date visited: 22.11.2020.
- [8] Earth Observatory, NASA, “*Milutin Milankovitch (1879-1958)*”, 24.03.2000. Retrieved from: https://earthobservatory.nasa.gov/features/Milankovitch/milankovitch_2.php. Date visited: 08.10.2020.
- [9] A. Kher, “*What Causes Seasons on Earth?*”. Retrieved from: <https://www.timeanddate.com/astronomy/seasons-causes.html>. Date visited: 08.10.2020.
- [10] S. Helm, “*Hours of daylight vs latitude vs day of year with tropical and polar circles*”, 10.03.2020. Retrieved from: https://commons.wikimedia.org/wiki/File:Hours_of_daylight_vs_latitude_vs_day_of_year_with_tropical_and_polar_circles.svg. Date visited: 08.10.2020.

- [11] *Traktat mellem Norge, Amerikas Forente Stater, Danmark, Frankrike, Italia, Japan, Nederlandene, Storbritannia og Irland og de britiske oversjøiske besiddelser og Sverige angående Spitsbergen [Svalbardtraktaten]*, 1920. Retrieved from: <https://lovdata.no/dokument/NL/lov/1920-02-09>. Date visited: 10.11.2020.
- [12] Google, “*Google Earth*”. Retrieved from <https://earth.google.com/web/>. Date visited: 10.11.2020.
- [13] Norsk Polarinstitutt, “*TopoSvalbard*”. Retrieved from: <https://toposvalbard.npolar.no/>. Date visited: 10.11.2020.
- [14] N. P. Thuesen, S. Barr, “Svalbard”, *Store Norske Leksikon*, 09.11.2020. Retrieved from: <https://snl.no/Svalbard>. Date visited: 15.9.2020.
- [15] T. Reid, “*Nuclear Power at McMurdo Station, Antarctica*”, 21.03.2014. Retrieved from: <http://large.stanford.edu/courses/2014/ph241/reid2/>. Date visited: 28.11.2020.
- [16] E.S. Viseth, Teknisk Ukeblad, “*Må forby solceller og vindkraft på Svalbard. Prisen tvinger fram dieselmotorkraftverk*”, 13.11.2018. Retrieved from: <https://www.tu.no/artikler/ma-forby-solceller-og-vindkraft-pa-svalbard-prisen-tvinger-fram-dieselmotorkraftverk/450723>. Date visited: 10.11.2020.
- [17] C. T. Decker et al., “*Opportunities for Waste Heat Recovery at Contingency Bases*”, ERDC, Washington DC, USA, ERDC/CERL TR-16-3 0. April 2016.
- [18] B. Jabeck, “The Impact of Generator Set Under loading”, CAT, LEXE0832-01, October 2014. Retrieved from: https://www.cat.com/en_AU/articles/The-impact-of-generator-set-underloading.html. Date visited: 11.11.2020.
- [19] B. Tennbakk et al., “Alternativer for framtidig energiforsyning på Svalbard”, Tema and Multiconsult, Olje- og Energidepartementet, ISBN nr. 978-82-8368-030-0, June 2018.
- [20] R.N. Andreassen, NRK, “*Utslippsrekord i Longyearbyen – slapp i fjor ut like mye CO₂ som 40.000 bensinbiler*”, 30.05.2020. Retrieved from: <https://www.nrk.no/tromsogfinnmark/utslippsrekord-i-longyearbyen--slapp-i-fjor-ut-like-mye-co--som-40.000-bensinbiler-1.15031609>. Date visited: 03.09.2020.

- [21] B. F. Johansen, J. Henriksen, Ø. Overrein, K. Prestvold, “*Ny-Ålesund (78° 55' N 11° 55' Ø)*”, Archived 09.12.2007. Retrieved from: <https://web.archive.org/web/20071209103654/http://cruisehandboka.npolar.no/Kongsfjorden/Ny-Alesund>. Date visited: 18.09.2020.
- [22] S. Merlet, “Opportunities for Solar Power in Ny-Ålesund”, Multiconsult, 128608-RIEn-RAP-01, 17.12.2018.
- [23] M. A. Fahim, T.A. Alsahhaf, A. Elkilani, “Chapter 2 - Refinery Feedstocks and Products”, *Fundamentals of Petroleum Refining*, 2010, p. 11-31. doi: 10.1016/B978-0-444-52785-1.00002-4.
- [24] IOR Energy, “*Engineering Conversion Factors*”, archived 25.09.2010. Retrieved from: <https://web.archive.org/web/20100825042309/http://www.ior.com.au/ecflist.html>. Date visited: 02.12.2020.
- [26] D. R. Williams, NASA, “*Sun Fact Sheet*”, 23.02.2018. Retrieved from: <https://nssdc.gsfc.nasa.gov/planetary/factsheet/sunfact.html>. Date visited: 24.11.2020.
- [25] C. Honsberg, S. Bowden, PVEducation, “*Solar Cell Structure*”. Retrieved from: <https://www.pveducation.org/pvcdrom/solar-cell-operation/solar-cell-structure>. Date visited: 13.12.2020.
- [27] D. R. Williams, NASA, “*Earth Fact Sheet*”, 24.11.2020. Retrieved from: <https://nssdc.gsfc.nasa.gov/planetary/factsheet/earthfact.html>. Date visited: 24.11.2020.
- [28] National Institute of Standards and Technology, “*Stefan-Boltzmann constant σ* ”. Retrieved from: <https://physics.nist.gov/cgi-bin/cuu/Value?sigma>. Date visited: 24.11.2020.
- [29] C. Honsberg, S. Bowden, PVEducation, “*Standard Solar Spectra*”. Retrieved from: <https://www.pveducation.org/pvcdrom/appendices/standard-solar-spectra>. Date visited: 24.11.2020.
- [30] C. Honsberg, S. Bowden, PVEducation, “*Air Mass*”. Retrieved from: <https://www.pveducation.org/pvcdrom/properties-of-sunlight/air-mass>. Date visited: 24.11.2020.

- [31] F. Kasten, A. T. Young, “Revised optical air mass tables and approximation formula”, *Applied Optics*, vol. 28, p. 4735–4738, 1989. doi: 10.1364/AO.28.004735.
- [32] PVPerformance, “*Global Horizon Irradiance*”. Retrieved from: <https://pvpmc.sandia.gov/modeling-steps/1-weather-design-inputs/irradiance-and-insolation-2/global-horizontal-irradiance/>. Date visited: 24.11.2020.
- [33] J. Skaar, “Albedo”, *Store Norske Leksikon*, 26.11.2020. Retrieved from: <https://snl.no/albedo>. Date visited: 24.11.2020.
- [34] Silicon Solar, “*What are Standard Test Conditions (STC)*”. Retrieved from: <https://www.siliconsolar.com/what-are-standard-test-conditions-stc/>. Date visited: 25.11.2020.
- [35] C. Honsberg, S. Bowden, PVEducation, “*Effect of Temperature*”. Retrieved from: <https://www.pveducation.org/pvcdrom/solar-cell-operation/effect-of-temperature>. Date visited: 25.11.2020.
- [36] Green Tech Media, “*Bifacial Plus Tracking Boosts Solar Energy Yield by 27 Percent*”, 18.04.2018. Retrieved from: <https://www.greentechmedia.com/articles/read/bifacial-plus-tracking-boosts-solar-energy-yield-by-27-percent#gs.wLGHoLY>. Date visited: 03.10.2020.
- [37] G. Masson, A. Detollenaere, J. V. Wetter, I. Kaizuka, A. Jäger-Waldau, J. Dunoso, “*Snapshot of Global PV Markets 2020*”, IEA PVPS TCP, ISBN 978-3-906042-94-7, April 2020.
- [38] N. Hall, NASA, “*First Law of Thermodynamics*”, 05.05.2015. Retrieved from: <https://www.grc.nasa.gov/www/k-12/airplane/thermo1.html>. Date visited: 03.10.2020.
- [39] Battery University, “*BU-205: Types of Lithium-ion*”, 03.12.2020. Retrieved from: https://batteryuniversity.com/learn/article/types_of_lithium_ion. Date visited: 13.11.2020.
- [40] Research Interfaces, “*Lithium-ion batteries for large-scale grid energy storage*”, 14.04.2018. Retrieved from: <https://researchinterfaces.com/lithium-ion-batteries-grid-energy-storage/>. Date visited: 13.11.2020.

- [41] I. Sarbu, C. Sebarchievici, “A Comprehensive Review of Thermal Energy Storage”, *Sustainability* 2018, vol. 10, p. 191, 14.01.2018. doi: 10.3390/su10010191.
- [42] K. Deng, K. Zhang, X. Xue, H. Zhou, “Design of a New Compressed Air Energy Storage System with Constant Gas Pressure and Temperature for Application in Coal Mine Roadways”, *Energies* 2019, vol. 12, p. 4188, 02.11.2019. doi: 10.3390/en12214188.
- [43] J. Wang et al., “Overview of Compressed Air Energy Storage and Technology Development”, *Energies* 2017, vol. 10, p. 991, 13.07.2017. doi: 10.3390/en10070991.
- [44] C. Meyer, “This is Svalbard 2016 What the figures say”, Statistisk Sentralbyrå, December 2019.
- [45] O. C. Kopp, Britannica, “*Overview of Compressed Air Energy Storage and Technology Development*”. Retrieved from: <https://www.britannica.com/science/coal-fossil-fuel/Structure-and-properties-of-coal>. Date visited: 03.10.2020.
- [46] P. Ralon et al., “*Electricity Storage and Renewables: Costs and Markets to 2030*”, IRENA, Abu Dhabi, ISBN 978-92-9260-038-9, October 2017.
- [47] United States Nuclear Regulatory Commission, “*Capacity factor (net)*”, 24.08.2020. Retrieved from: <https://www.nrc.gov/reading-rm/basic-ref/glossary/capacity-factor-net.html>. Date visited: 19.09.2020.
- [48] U.S. Energy Information Administration, “*Table 6.07.A. Capacity Factors for Utility Scale Generators Primarily Using Fossil Fuels*”. Retrieved from: https://www.eia.gov/electricity/monthly/epm_table_grapher.php?t=epmt_6_07_a. Date visited: 19.09.2020.
- [49] DBEIS, “*DIGEST OF UNITED KINGDOM ENERGY STATISTICS 2020*”, 2020. Retrieved from: <http://www.decc.gov.uk/assets/decc/11/stats/publications/dukes/5955-dukes-2012-chapter-5-electricity.pdf>. Date visited: 19.09.2020.
- [50] U.S. Energy Information Administration, “*Table 6.07.B. Capacity Factors for Utility Scale Generators Primarily Using Non-Fossil Fuels*”. Retrieved from:

https://www.eia.gov/electricity/monthly/epm_table_grapher.php?t=epmt_6_07_b. Date visited: 19.09.2020.

[51] H. With et al., “Recent Facts about Photovoltaics in Germany”, Fraunhofer ISE, 10.06.2020. Retrieved from: <https://www.ise.fraunhofer.de/content/dam/ise/en/documents/publications/studies/recent-facts-about-photovoltaics-in-germany.pdf>. Date visited: 19.09.2020.

[52] Avinor, “Svalbard Airport”. Retrieved from: <https://avinor.no/en/airport/svalbard-airport/>. Date visited: 21.09.2020.

[53] Avinor, “Luftfartens Utslipp”. Retrieved from: <https://avinor.no/en/corporate/klima/klimagassutslipp/>. Date visited: 21.09.2020.

[54] Avinor, “Annual and sustainability report 2019”, Oslo, Norway, 31.03.2020.

[55] Time and Date, “Longyearbyen, Svalbard, Norge — Soloppgang, solnedgang og dagens lengde, august 2020”. Retrieved from: <https://www.timeanddate.no/astronomi/sol/norge/longyearbyen?month=8&year=2020>. Date visited: 21.09.2020.

[56] Time and Date, “Longyearbyen, Svalbard, Norge – Soloppgang, solnedgang og dagens lengde, juni 2020”. Retrieved from: <https://www.timeanddate.no/astronomi/sol/norge/longyearbyen?maaned=6&year=2020>. Date visited: 21.09.2020.

[57] Peakfinder, “View from Svalbard Airport, September 14th, 2020”. Retrieved from: <https://www.peakfinder.org/?lat=78.2466&lng=15.495&azi=181&zoom=4&ele=27&cfg=s&date=2020-09-15T06:57Z&name=Svalbard%20Airport>. Date visited: 23.09.2020.

[58] Weather Spark, “Average Weather at Svalbard Airport, Longyear”. Retrieved from: <https://weatherspark.com/y/148359/Average-Weather-at-Svalbard-Airport-Longyear;-Svalbard-&-Jan-Mayen-Year-Round>. Date visited: 10.11.2020.

- [59] P. Strøm, Y. Schwenke, NRK, “*Slo 41 år gammel varmere rekord på Spitsbergen*”, 26.07.2020. Retrieved from: <https://www.nrk.no/tromsogfinnmark/slo-41-ar-gammel-varmere-rekord-pa-spitsbergen-1.15100814>. Date visited: 10.11.2020.
- [60] Avinor, “Års- og samfunnsansvarsrapport”, Oslo, Norway, 29.03.2017.
- [61] T. O. Enoksen, “Evaluation of a Solar Power Plant at Longyearbyen”, Master’s Thesis in Energy, Climate and Environment, Faculty of Science and Technology, Department of Physics and Technology, University of Tromsø, Tromsø, June 2020.
- [62] M. Schachinger, PVXchange, “*Market Analysis November - 2020 was off to a good start, and then ...*”, 24.11.2020. Retrieved from: <https://www.pvxchange.com/en/news/price-index>. Date visited: 03.12.2020.
- [63] Sunpower, “SunPower® E-Series Residential Solar Panels | E20-327”, December 2016. Retrieved from: <https://us.sunpower.com/sites/default/files/media-library/data-sheets/ds-e20-series-327-residential-solar-panels.pdf>. Date visited: 25.09.2020.
- [64] Jinko Solar, “JKM265P-60 245-265 Watt POLY CRYSTALLINE MODULE”. Retrieved from: <http://www.off-grid.at/wp-content/uploads/2020/04/Jinko-245-260W.pdf>. Date visited: 25.09.2020.
- [65] Fronius, “*Fronius Symo*”. Retrieved from: <https://www.fronius.com/en-gb/uk/photovoltaics/products/all-products/inverters/fronius-symo/fronius-symo-3-0-3-m>. Date visited: 28.09.2020.
- [66] Ø Kleven, H. Persson, C. Good, W. Sulkowski, T. Boström, “Solar Cells Above the Arctic Circle - a Comparison between a Two-Axis Tracking System and Simulations”, presented at the 24th European Photovoltaic Solar Energy Conference (EUPVSEC), Hamburg, Germany, September 2009.
- [67] Regjeringa, “*Statsbudsjettet 2021: Regjeringa vil dekkje driftsunderskottet i Gruve 7 på Svalbard*”, 07.10.2020. Retrieved from: <https://www.regjeringen.no/no/aktuelt/regjeringa-vil-dekkje-driftsunderskottet-i-gruve-7-pa-svalbard/id2769019/>. Date visited: 01.12.2020.

- [68] Longyearbyen Lokalstyre, “Handlingsprogram og økonomiplan 2020 – 2023 Budsjett 2020”, 09.12.2019.
- [69] L. N. Ylvisåker, High North News, “Statsbudsjettet 2021 – Longyearbyen lokalstyre får auka handlingsrom”, 07.10.2020. Retrieved from: <https://www.highnorthnews.com/nb/longyearbyen-lokalstyre-far-auka-handlingsrom>. Date visited: 01.12.2020.
- [70] Longyearbyen Lokalstyre, “Gebyr- og fakturasatser 2020 for Longyearbyen lokalstyre”, 09.12.2020.
- [71] Toll Customs, “Importkalkulator”. Retrieved from: <https://www.toll.no/no/verktoy/importkalkulator/>. Date visited: 01.12.2020.
- [72] Toll Customs, “Tollfritak for varer fra særlige områder”. Retrieved from: <https://www.toll.no/no/verktoy/regelverk/tollabc/5/5-4/tollfritak-for-varer-fra-sarlige-omrader/>. Date visited: 01.12.2020.
- [73] Investing, “EUR/NOK – Euro Norwegian Krone”, 01.12.2020. Retrieved from: <https://www.investing.com/currencies/eur-nok-historical-data>. Date visited: 01.12.2020.
- [74] Trading Economics, “Norway Inflation Rate”. Retrieved from: <https://tradingeconomics.com/norway/inflation-cpi>. Date visited: 10.11.2020.
- [75] M. Schachinger, PVXchange, “Market Analysis July 2017 - Origin must not be a factor - only quality should count!”, 25.07.2017. Retrieved from: <https://www.pvxchange.com/en/market-analysis-july-2017-origin-must-not-be-a-factor-only-quality-should-count>. Date visited: 03.12.2020.
- [76] S. Schlömer et al., “Annex III: Technology-specific cost and performance parameters. In: Climate Change 2014: Mitigation of Climate Change. Contribution of Working Group III to the Fifth Assessment Report of the Intergovernmental Panel on Climate Change”. Cambridge University Press, Cambridge, United Kingdom and New York, NY, USA, 2014. Retrieved from: https://www.ipcc.ch/site/assets/uploads/2018/02/ipcc_wg3_ar5_annex-iii.pdf. Date visited: 04.12.2020.

[77] Coal Marketing International LTD, “*Coal Basics*”. Retrieved from:
<http://www.coalmarketinginfo.com/coal-basics/>. Date visited: 04.12.2020.

[78] T. W. Davies, “*Calculation of CO₂ emission from fuels*”, 2005. Retrieved from:
https://people.exeter.ac.uk/TWDavies/energy_conversion/Calculation%20of%20CO2%20emissions%20from%20fuels.htm. Date visited: 04.12.2020.

[79] H. K. Ringkjøb, P. M. Haugan, A. Nybø, “*Transitioning remote Arctic settlements to renewable energy systems – A modelling study of Longyearbyen, Svalbard*”, *Applied Energy* vol. 258, 15.01.2020, art. no. 114079. doi: 10.1016/j.apenergy.2019.114079.

